# UC San Diego
## UC San Diego Electronic Theses and Dissertations

**Title**

Developing cell based reporters for the investigation of human pluripotent stem cell derived Müller Glia

**Permalink**

https://escholarship.org/uc/item/6dc633dr

**Author**

Su, Fei

**Publication Date**

2018

Peer reviewed|Thesis/dissertation

UNIVERSITY OF CALIFORNIA SAN DIEGO

Developing cell based reporters for the investigation of human pluripotent stem cell derived

Müller Glia

A Thesis submitted in partial satisfaction of the requirements for the degree Master of Science

in

Biology

by

Fei Su

Committee in charge:

      Professor Karl J. Wahlin, Chair
      Professor George P. Fortes, Co-Chair
      Professor Julian I. Schroeder

2018

The Thesis of Fei Su is approved, and it is acceptable in quality and form

for publication on microfilm and electronically:

_____

_____

Co-Chair

_____

Chair

University of California San Diego

2018

# Table of Contents

List of Abbreviations

| | |
|---|---|
| 2D | 2-Dimensional |
| 3D | 3-Dimensional |
| AAV | Adeno-associated Virus |
| AAVS1 | Adeno-Associated Virus Integration Site 1 |
| ASCL1 | Achaete-Scute Family BHLH Transcription Factor 1 |
| ATRA | All-trans Retinoic Acid |
| Brn3b | Brain-Specific Homeobox 3b |
| CAG | Chicken ß-actin Promoter |
| CBH | Hybrid form of Chicken ß-actin Promoter |
| cDNA | Complementary Deoxyribonucleic acid |
| CLYBL | Citrate Lyase Beta-Like |
| CNS | Central Nervous System |
| CRISPR | Clustered Regularly Interspaced Short Palindromic Repeats |
| CRISPRa | Clustered Regularly Interspaced Short Palindromic Repeats activation |
| CRISPRi | Clustered Regularly Interspaced Short Palindromic Repeats interference |
| Crx | Cone-Rod Homeobox |
| DMEM | Dulbecco Modified Eagle Medium |
| DMSO | Dimethyl sulfoxide |
| DNA | Deoxyribonucleic acid |
| dPBS | Dulbecco's Phosphate Buffered Salin |
| E6 | Essential 6 Medium |
| EGFP | Enhanced Green Fluorescent Protein |
| ESC | Embryonic Stem Cell (human) |
| GFAP | Glial Fibrillary Acidic Protein |
| GLAST | Glutamate Aspartate Transporter |
| GLUL | Glutamate-Ammonia Ligase |
| H2B | Histone 2 Binding Protein |

| | |
|---|---|
| H9 | WA09 (H9) Human Embryonic Stem Cell Line |
| HIFI | High Fidelity |
| hRPL30 | Human L Ribosomal Proteins 30 |
| IMR90.4 | IMR90.4 Human Induced Pluripotent Stem Cell line |
| iPSC | Induced Pluripotent Stem Cell (human) |
| Klf4 | Kruppel Like Factor 4 |
| LTR | Long-term maintenance media |
| M | Molar |
| MC | Minicircle |
| MNU | N-methyl-N-nitrosourea |
| mRNA | Messenger Ribonucleic Acid |
| NLS | Nuclear Localization Signal |
| nM | Nanomolar |
| NMDA | N-Methyl-D-aspartic acid |
| Oct3 or 4 | Octamer-Binding Transcription Factor 3 or 4 |
| Otx2 | Orthodenticle Homeobox 2 |
| P2A | 2A peptide |
| POU4F2 | POU Class 4 Homeobox 2 |
| RNA | Ribonucleic Acid |
| SAG | Smoothened Agonist |
| SLC1A3 | Solute Carrier Family 1 Member 3 |
| Sox2 | Sex Determining Region Y-box 2 |
| SV40/SV40-PA | Simian virus 40 PolyA |
| tdTomato | Tandem Dimeric Tomato fluorescent protein |
| µL | Microliter |
| µM | Micromolar |
| µm | Micrometer |

List of Figures

# List of Schematics

# List of Tables

Acknowledgements

This thesis, in part is currently being prepared for submission for publication of the

material. Su, Fei; Wahlin, Karl. The thesis author was the primary investigator and author of this

material.

Abstract of the Thesis


Developing cell based reporters for the investigation of human pluripotent stem cell derived

Müller Gila


by


Fei Su

Masters of Science in Biology

University of California San Diego, 2018


Professor Karl J. Wahlin, Chair
Professor George P. Fortes, Co-Chair


Retinal neuron degenerations of an eye can result in permanent photoreceptor or retinal ganglion cell loss which leads to permanent blindness. One potential approach to restore vision loss is through transplanting stem cell or stem cell-derived retinal neurons into the sub-retinal space of the injured retina. However, these transplanted cells often fail to integrate or form a functional connections with the neighboring retinal neurons. Another alternative approach is

referred to as the endogenous regeneration whereby new retinal neurons are generated from Müller glia to replace those lost photoreceptors and retinal ganglion cells. Müller glia is the only cell in the retina that shares a common origin with retinal neurons. Thus it has the potential to convert into retinal neurons. Studies have shown that Müller cells in fish, amphibians, and chickens in early developmental stage respond to injury, triggering *in vivo* regeneration of retinal neurons. In mammals this form of regeneration is less common but does appear to occur as well, however, it remains to be determined whether human Müller glia can dedifferentiate into retinal progenitor and regenerate retinal neurons. Therefore, my project aims to establish Müller cell specific fluorescent reporter systems to aid in future Müller Glia endogenous studies. One approach is to build a dual reporter system that tags both retinal ganglion cells and Müller Glia, tracking the exact time point at which Müller cells are developed from iPSCs. The other approach is to use a lineage tracing system and permanently tag Müller cells once they are born. The advantage of the lineage tracer system is that even if Müller cells convert into other cell types, the fluorescent markers will continue to be expressed, therefore indicating their Müller Glia origin.

Introduction

Human retinal neuron loss is commonly seen in variable ocular diseases, including retinitis pigmentosa, glaucoma, and age-related macular degeneration. Blunt trauma, open globe penetration or non-penetrating injury can also lead to damage on retinal neurons, particularly photoreceptors and ganglion cells which are necessary for converting light energy into electric signals and for transmitting those visual signals to the back of the brain respectively. Since cell loss often leads to permanent blindness, people have focused their attention on stem cell transplantation therapy. Two major types of pluripotent stem cells exist: embryonic stem cell and induced pluripotent stem cell. Embryonic stem cells (ESCs) are stem cell lines separated from blastomeres during early human embryo development after fertilization treatment *in vitro*. It is considered pluripotent since it can develop into all kinds of different cell types in the human body, except the placenta. ESCs' potential of generating human tissue cells had broadly expanded their usage in research fields. Study of human cells *in vitro* no longer requires painful extraction of samples from patients or deceased people under the risk of moral issue. Hence, embryonic stem cells had become a prominent reference for tracking early human development in research studying, disease modeling, drug screening or teratogenicity testing (Nichols, 2001).

The other type of pluripotent stem cell is the induced pluripotent stem cell (iPSC), which is generated through exposure of somatic cells to proteins encoding transcription factors that are expressed in iPSCs. This approach was pioneered by Takahashi and Yamanaka who demonstrated that through retroviral transduction of only 4 protein coding sequences: *Oct3 /4, Sox2, c-Myc,* and *Klf4,* fibroblasts could be converted into cells with remarkable similarity to ESCs (Takahashi and Yamanaka, 2006). These iPSC can differentiate into all three germ layers, including neural tissues, cartilage, and columnar epithelium. Like ESCs, iPSC pluripotency is not

affected by repeated passaging and can give rise to each of the three germ layers, demonstrating their utility as a model for studying embryonic development *in vitro*.

Currently, there are two approaches to replace impaired retinal neurons using stem cell lines mentioned above: one is to directly inject stem cells into the vitreous chamber of the injured retina. After a few weeks, these stem cells are able to migrate to various retinal layers and express corresponding retinal neuron specific markers (Castanheira et al., 2008). Other approach involves expanding and differentiate stem cells into retinal neurons *in vitro* first, then proceed to transplantation (Chao et al., 2017). Either way will inevitably introduce an open wound on the eyeball, followed by risks of infection, scarring, or even tumorgenesis. Moreover, several technical drawbacks remain: the integration of stem cell-derived retinal neurons into the complex structure of retina is already a technical challenge, to ensure their functionality to transmit and receive electric signal is even more so.

Given these limitations, endogenous regeneration was proposed as an alternative to bypass these invasive procedures. Endogenous regeneration aims to use retinal Müller cells that have the regenerative potential to replenish lost photoreceptors and ganglion cells. Müller Glia, contribute approximately 90% of retinal glia, spans the width of the retina with nuclei residing in the inner nuclear layer. Other retinal glial cell types include astrocytes and microglial cells. While astrocytes have a flattened and outstretched cell body and surround blood vessels, microglial are resident macrophages that exhibit altered morphology and position depending on their activation status (Vecino et al., 2016) (Schematic 1).

**Müller Glia**     **Retinal Astrocyte**          **Microglia**
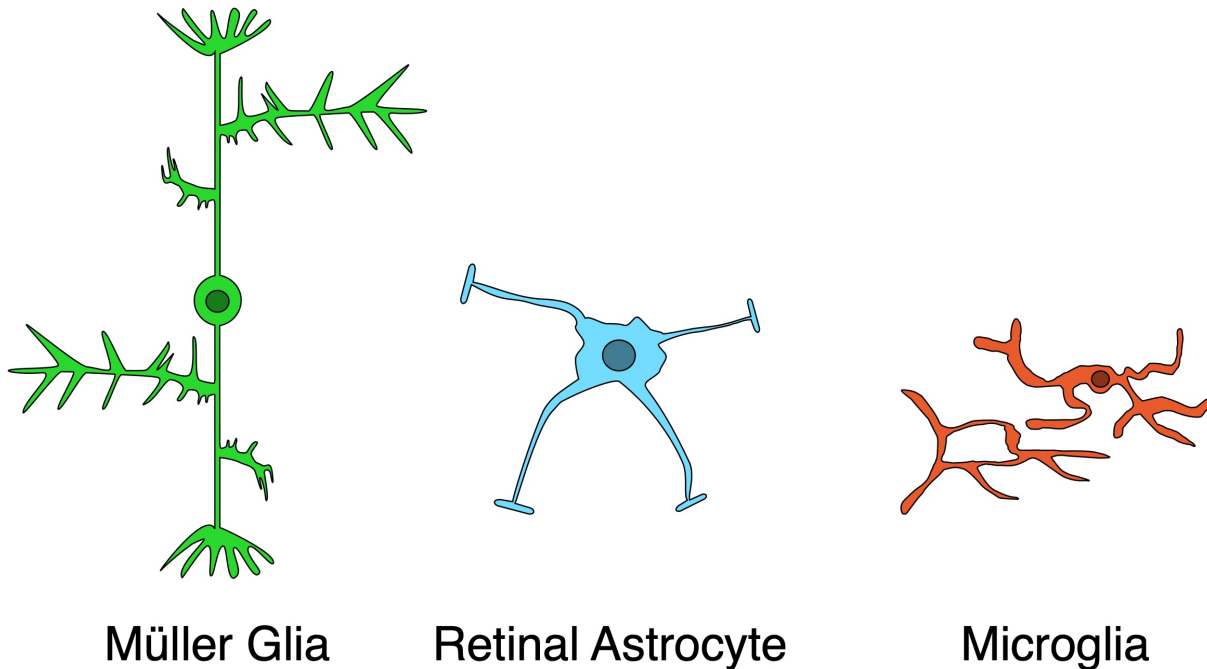
Schematic 1. Schematic drawing of the morphology of different types of retinal glial cells. Müller Glia has long cell body with microvilli extending to other layers of the retina. Retinal astrocyte spread its cell body that sheaths the blood vessel. Microglia have a fork shaped cell body and a rather big nucleus in its "resting" state; its morphology becomes ameboid-like, exhibiting pseudopodia.

In general, retinal glial cells share some functional similarities, including the formation of a protective boundaries to prevent foreign object invasion to the retina, providing structural support for neighboring neurons, stockpiling energy for neuron metabolism, generating extracellular matrix as a vital source of supporting and signaling factors in the retina, regulating neuronal activity and synaptic networks and activating immune responses to invading pathogens (Vecino et al., 2016). Müller Glia have several noteworthy differences. Importantly, they share a common origin with retinal neurons. It becomes reactive in response to retinal injury and diseases and undergo morphological, biological and molecular level changes. This stress-response process is often called reactive gliosis, which involves three steps: proliferation, dedifferentiation, and regeneration. Among those three steps, proliferation is not always seen in

reactive gliosis, but the triggers for reactive gliosis are currently unknown. Fish, amphibians and early development chicken had shown Müller Glia responding to injuries and ability to reform lost retinal neurons after a few days to a few weeks (Goldman, 2014). Teleost fish, especially zebrafish, can restore impaired retina with retinal neurons and regain fully functional vision. Studies have shown that proliferating Müller Glia in zebrafish can generate rod photoreceptors when directed into such fate by targeting particular genomic sequences (Yao et al., 2018). Nonetheless, mammals, especially moving up along the phylogenic tree, have already lost this ability to regenerate retinal neurons (Goldman, 2014).

Recent studies have been conducted using mouse models in an effort to drive Müller glia to dedifferentiate into retinal progenitor followed by generation of photoreceptors and ganglion cells. Studies have shown Müller glia in mice is able to generate both neurons and glial cells. When transplanted into damaged rodent retina, primary human Müller Glia cells displayed regenerative potential and generated photoreceptors and retinal ganglion cells (Goldman, 2014). Therefore, it is reliable to conclude that Müller Glia, in general, has the capability to regenerate retinal neurons under proper circumstances. Unfortunately, scientists have struggled to trigger Müller Glia regeneration *in vivo*. A drug-induced injury is able to activate the ability of Müller Glia in mammal in proliferation and regeneration, but the probability of such event is rare. NMDA, a drug commonly used to impair live neurons, treated to mice retina led to some proliferative event in Müller cells, but the percentage of proliferating cells is very low (Ooto et al., 2004). Other study used MNU injection into mice that had successfully induced reactive gliosis, but the following regeneration process was slow and unstable, marked by the disappearance and reappearance of a regenerated retinal neuron marker seven days after the

treatment (Wan et al., 2008). Several pathways, including *Wnt-beta-catenin*, *Sonic Hedgehog*

and *ASCL1*, have been found to have effects on Müller Glia proliferation *in vitro*, which is the

first step to reactive gliosis (Goldman, 2014).

Despite some degree of success in many model organisms, Müller cell retinal regeneration

remains unexplored. One main reason is that human retinal development takes far longer for

maturation as compared to mice or other species. Horizontal, amacrine, ganglion, and cone cells

are the first cells to be generated during embryonic development, with rods and bipolar cells are

generated after, and Müller Glia usually occurs the last. Secondly, tracking human retinal

development is far more challenging comparing to tracking mice's. Due to ethical and technical

difficulties, one can only monitor human retina differentiation from stem cells *in vitro*, either as

flattened 2D culture or floating 3D mini-retinas. Past studies have shown that by regulating

several pathways, stem cells can be driven toward ectoderm and even into a retinal fate through

activation of the *Wnt* and *Hedgehog* pathways (Marquardt and Gruss, 2002). The approximate

time of mouse and human retinal neuron development is shown below (Marquardt and Gruss,

2002) (Schematic 2). In human retinal development *in vitro*, however, only the time point when

each type of retinal neurons appears can be determined. Usually this process involves tagging

cryosections of retinal organoids developed *in vitro* extracted at different time points with retinal

neuron-specific markers. Retinal ganglion cells are the first to be generated from iPSCs at around

28 to 36 days after germination. Horizontal cell-specific marker showed positive soon after, at

approximately day 40 to day 50. Bipolar cells, rods, and cones are generated from iPSCs roughly

at the same time as horizontal cells, with a slight difference in time. Amacrine cells are not

generated until day 70. Müller Glial cells are the last to be developed from iPSCs-developed

retinal progenitors, usually not until after day 90. Nonetheless, all retinal neurons in human will continue to develop, even after birth and up until 5 years later (Llonch et al., 2018). Hence human retinal developmental study is a long and expensive process, without a proper tool that constitutively track the generation process of retinal neurons.
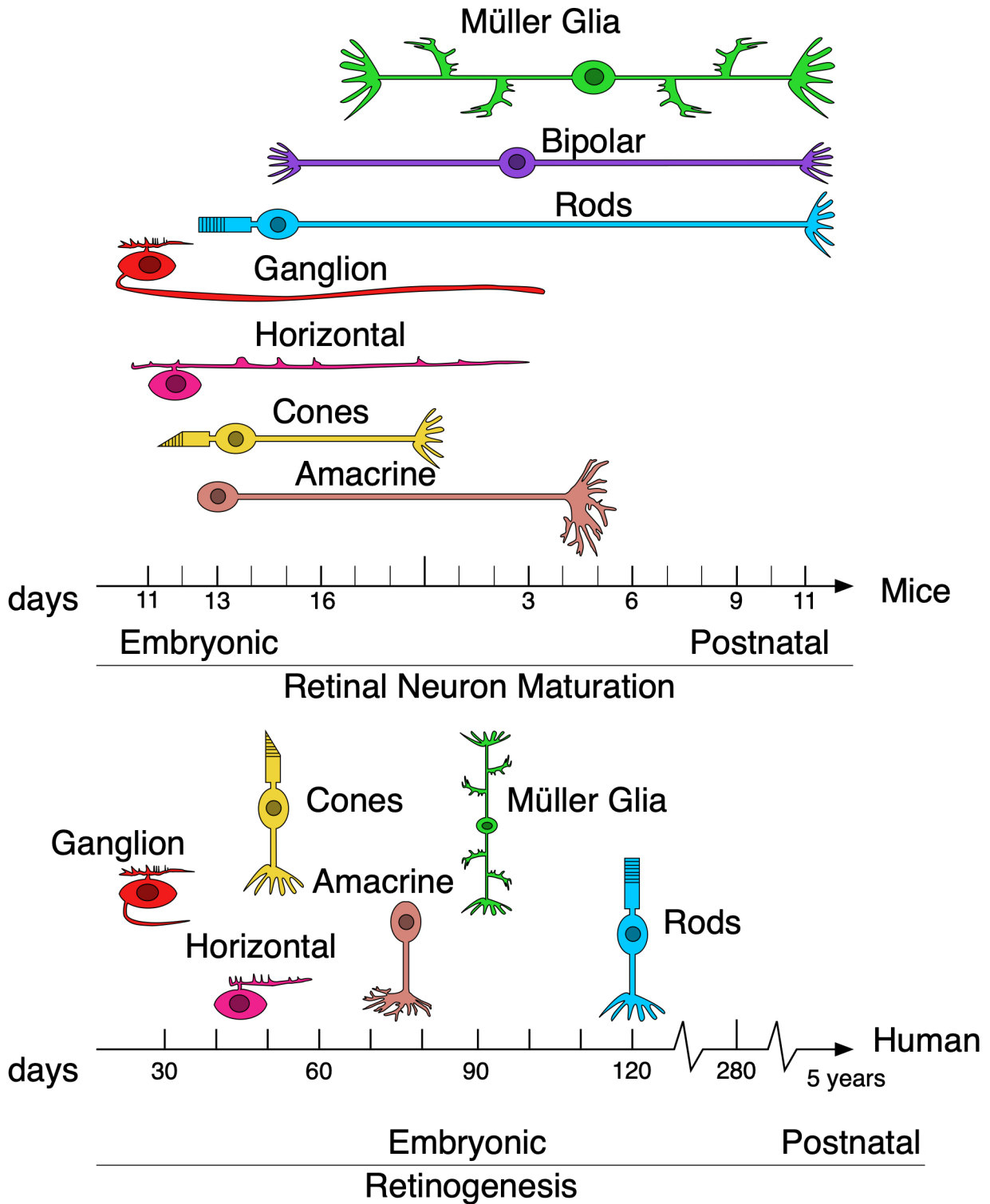
Schematic 2. Timeline of retinal neuron development in mouce and time point of when each retinal neurons are generated in human. The length of each neuron represents the time period when these cells are generated. Retinal neuron development of mouse extends to after fetal mice were born. Human retinal development is shown in individual time points only, indicating when each retinal neurons were born. The time period of human retinal development remained unclear.

8

The insert of cell birth for Müller Glia are more challenging. Firstly, the exact period when human Müller Glia is first generated is currently unknown. Researchers were only able to identify various Müller cell markers expressed in human fetal retina (Walcott and Provis, 2003). Photoreceptors in human do not mature until after approximately 30-90 days, meaning Müller glial cells can only occur after that time period (Wahlin et al., 2017). Secondly, researchers had been using immuno-labeling cryosections of fetal retina collected from different ages with antibodies binding to Müller cell-specific pathway to visualize Müller cell marker expression level (Walcott and Provis, 2003). An alternative way to target and express Müller cell-specific markers is to use AAV with potential Müller Glia marker-specific promoters to drive GFP expression to identify Müller cell markers and their expression level in live Müller Glia (Pellissier et al., 2014). However, there has not been a live-cell-development-tracking fluorescent marker labeled Müller cell line to track real-time development from human stem cells *in vitro*.

Therefore, my study aims to develop a tool that tracks Müller Glia development throughout the retinal stem cell differentiation process. By tagging Müller Glia-specific markers with fluorescent proteins, we will be able to reliably monitor when and where muller cells first arise. Two approaches will be made to establish Müller Glia reporters: one is to build a dual reporter system tagging both *Brn3b*, a retinal ganglion cell marker, and *GLAST*, a protein highly expressed in mature human Müller Glial cells; the other is to build a lineage trace system which marks Müller cell origin once they are generated from differentiating retinal neural progenitors and after they develop into other cell types. The two systems mentioned above will be inserted into iPSC genome through a tetracycline-controlled transactivated CRISPR/Cas9 system that will

only generate activate Cas9 protein and its genomic editing function when treated with tetracycline or doxycycline, which both refer to chemical molecules that bind to corresponding response element on the genome and start Cas9 protein transcription (Tak et al., 2017). Doxycycline is a chemical that shares similar structure with tetracycline but it ensures higher efficiency on transcriptional activation (Campbell et al., 2012).

*Brn3b* is a transcription factor encoded by a brain-specific POU domain homeobox gene, *POU4F2*. It is a gene that down-regulates of a wide range of genes involving in retinal development, including *Dlx1 and Dlx2*, which the survival and differentiation of late-born retinal ganglion cells heavily depend on. An analysis on gene expression level changes in *Brn3b* knock out mice retinas exhibited a suppression of amacrine and horizontal cell development. Upregulation of *Otx2, Crx* and several other photoreceptor progenitor markers mRNA level in *Brn3b* knock out mice retina suggests an inhibitory effect of *Brn3b* on photoreceptor generation also. All of these above implied that *Brn3b* maintains a retinal ganglion cell fate by suppressing differentiation into other retinal neuronal cell types (Qiu et al., 2008). Therefore, a high level of *Brn3b* expression can be used to indicate retinal ganglion cell presence.

*GLAST*, on the other hand, is a glial cell-specific high-affinity $Na^+$-dependent Glutamine transporter, which is involved in the uptake of glutamine neurotransmitters. It is widely expressed in CNS during early development of the embryo. However, later its expression is limited gradually to radial glial cells in the cerebellum, the retina, and the olfactory bulb. Since Glutamine is a primary excitatory transmitter involved in photoreceptor-ganglion interaction In the retina, it becomes crucial to maintain Glutamine concentration at the synaptic cleft, which was aided by *GLAST* transporter in Müller cells (López-Colomé et al., 2016). Unlike *GFAP*, a

glial cell marker which is commonly seen in retinal astrocytes and microglial cells, *GLAST* is expressed in the mature retina exclusively in Müller cells (Vecino et al., 2016). Hence, *GLAST* is a preferential indicator for Müller glia cells. Building a dual reporter *Brn3b*-2A-tdTomato / *GLAST*-2A-eGFP system is significant for tracking human retinal neuron development from iPSCs since both markers are specifically expressed only in their corresponding cell types and the time point point at which they are expressed indicates the initial generation of ganglion cells or Müller glial cells, marking the maturation state of developing retina. Therefore, when studying an *in vitro* model of human stem cell differentiation, a dual-reporter system is able to help us better understand the exact time at which stage the developing retina is in (Schematic 3). In the dual system cassette, the H2B protein mainly serves to stabilize the fluorescent protein to the nucleus (Zolessi et al., 2006). The p2A is a self-cleaving peptide that separates the fluorescent tag from the cell protein to prevent the fluorescent protein from interfering the normal cell functions (Kim et al., 2011).
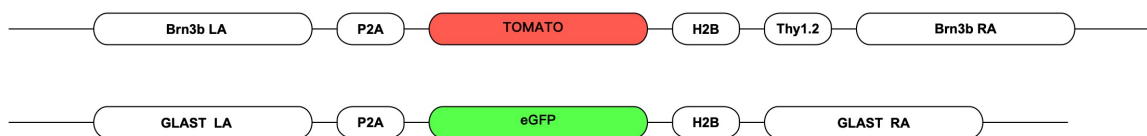


Schematic 3. Brn3b-GLAST dual reporter system in iPSC. P2A is a self-cleaving peptide that separates fluorescent protein from normal genomic expression product. H2B is a nuclear localization tag for fluorescent protein, reflecting cell nucleus position and morphology.

A derivative of this dual reporter system is based on lineage tracing (Schematic 4). Lineage tracing of cells was previously used in mice as a manner to knock down or knock out certain genes to study their corresponding genomic function *in vivo*. CRE recombinase, weight 38kDa, is able to cleave, invert, and replace particular genomic sequences by recognizing a 34bp loxP sequence flanking the target site (Oberdoerffer et al., 2003). In this lineage tracing system, CRE
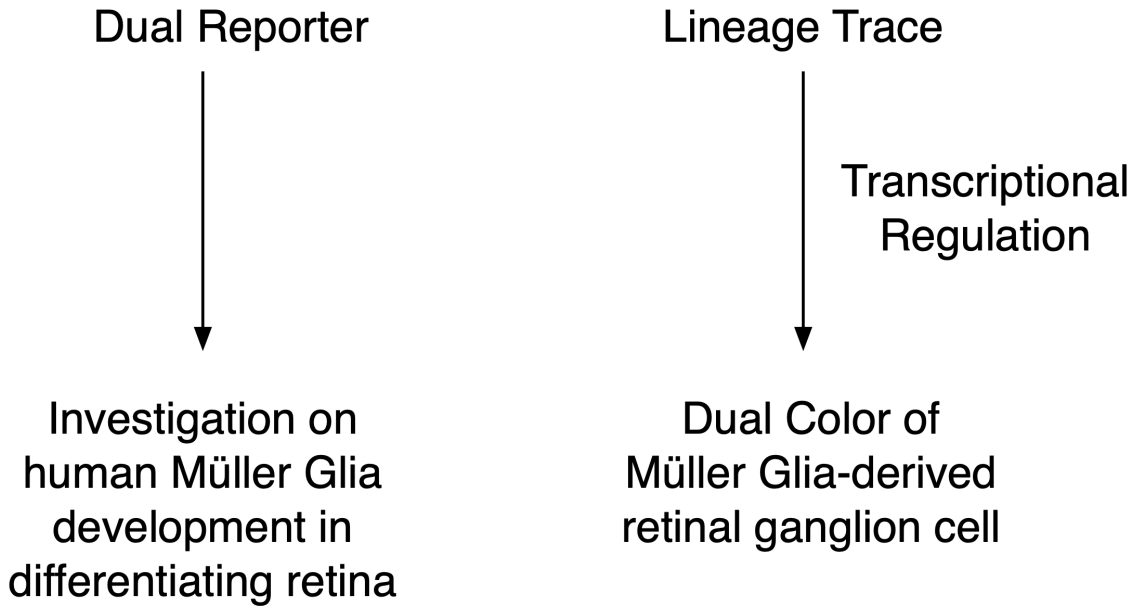
recombinase is used to remove a premature STOP site flanking a Ruby3 fluorescent protein coding sequence integrated into a safe harbor site. A safe harbor site is a locus in the genome that supports robust and stable transgene expression from integrated sites and is not affected by the structures or function of adjacent endogenous genes. It also must not affect the regular cellular activity or inadvertently affect cancerous gene or microRNA expression (Oberdoerffer et al., 2003). Widely used and studied safe harbor sites includes *AAVS1*, *H11*, and *hROSA26* (Cerbini et al., 2015). However, for iPSC used in this study, *AAVS1* site, the most commonly used and efficient one, is occupied by the tetracycline inducible CRISPR/Cas9 coding sequence mentioned above for genomic editing. Our lab previously observed that the *H11* site had diminished transgene expression after repeated passage and after stem cells underwent differentiation (unpublished data). Hence, alternative safe harbor sites must be sought out. In this thesis, a relatively novel safe harbor site located in the *Citrate Lyase Beta-Like* (*CLYBL*) gene was chosen. *CLYBL* was first applied in H9 ESCs and displayed robust expression at stem cell stage (Cerbini et al., 2015). When CRE finds the LoxP sites and removes the premature STOP site flanking the LoxP sequence, *CLYBL* will activate Cbh promoter driven Ruby3 fluorescent marker to be continuously expressed in *GLAST* activated cell, indicating a Müller Glia origin (Schematic 4). This system can become particularly useful when studying Müller cell-derived retinal progenitors and neurons. As Müller cells convert into other cell types, the newly regenerated cells would be expected to silence Müller cell specific genes leaving no reliable proof that new cells were differentiated from Müller cells. On the other hand, a lineage trace system would show constitutive expression in both muller cells or any cells that once were of

12

Muller cell origin. The Müller glia-derived neurons will carry this marker within their nucleus, hence pointing back to a Müller cell origin.
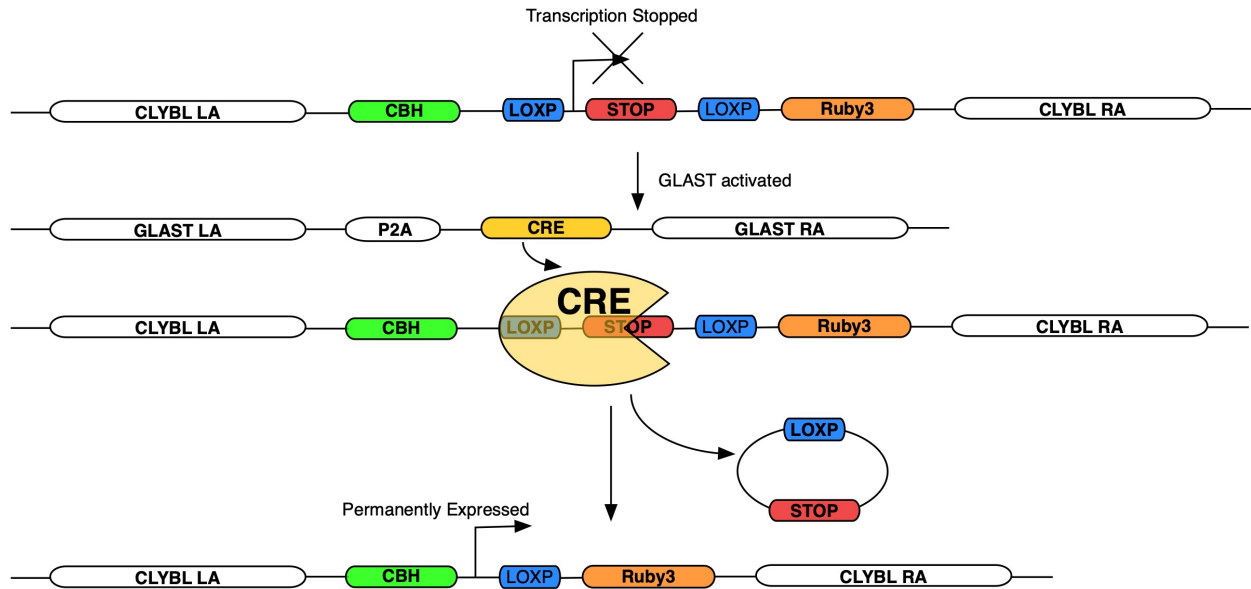


Schematic 4. Lineage trace system. GLAST-driven CRE recombinase cleaving LoxP flanking a STOP site, leads to permanent expression of Ruby3 fluorescent protein in the safe harbor genome locus.

Building these two systems for characterizing Müller Glia development is crucial for the following projects, which involves targeting particular pathways in Müller Glia, in an attempt to restore their regenerative potential. The fluorescent protein tagged *GLAST* cassette in the dual reporter system will set up a traceable series of time points on when the Müller Glia is generated during human retina development while the *Brn3b*-H2B-tdTomato cassette sets up an indicator for healthy, rightfully developed human retina. For photoreceptors or retinal ganglion cells differentiated from Müller Glia derived progenitor cells, Lineage tracing system becomes utterly important since it leaves a permanently expressed marker that is only activated when Müller Glia was generated (Schematic 5).

Dual Reporter                    Lineage Trace

|                                    Transcriptional
|                                    Regulation
↓                                    ↓

Investigation on                 Dual Color of
human Müller Glia                Müller Glia-derived
development in                    retinal ganglion cell
differentiating retina

Schematic 5. Future appliance of the Dual Reporter System and the Lineage Trace System. Cells that harbors either of those two systems can be used in tracking Müller Glia development in human or investigating transcriptional regulated Müller Glia regeneration.

Results

Transfected iPSC cells harboring *Brn3b-GLAST* dual reporter system were plated into 96 well U-bottom plate at low density (125 cells/well) for better nutritional feeding and larger space for cell division and proliferation. TsFGF was added to the iPSCs on day 0. Stem cells slowly aggregated under the effect of gravity and were subsequently treated with Matrigel during the first 5 days growing in hypoxia environment, while optic vesicles morphology could be seen under live confocal imaging using ImageXpress electronic microscopy imaging device (Figure 1; white arrows). The cells were then transferred to normoxia for long-term maintenance. Based on previous experience, the fluorescent protein expressed at later time points will have brighter intensity under this condition. On d11, multiple spherical optical vesicles occurred on the edges of round shaped aggregated retinal progenitor cell colonies, which were then cut out from each other using a pair of sharpened needles to prevent the center of the organoid from forming necrotic cores due to lack of nutrition. Separated organoids were maintained in 10cm polystyrene plates at low density with constant orbital shaking at a low speed (35-40 times/minute) to ensure media were evenly distributed to each organoid.
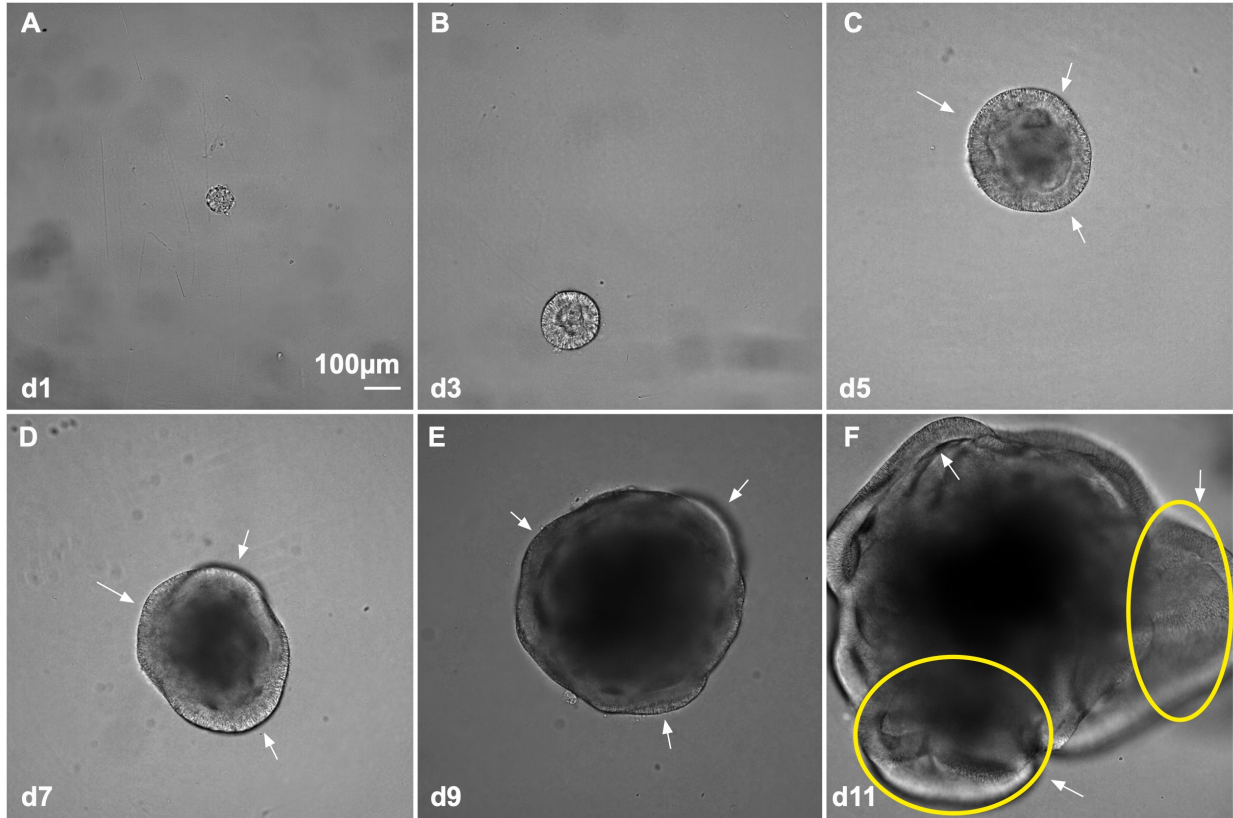
Figure 1. 10x images of iPSC differentiation from 2D stem cell culture to 3D floating retinal organoids from d1 to d11. The stem cell aggregates gradually forms layer of optic cup, as shown in white arrows pointing. On d11, clear morphology of optic vesicles can be seen, as shown in yellow circle. Scale bars = 100μm.

The organoids continued to develop as the retinal progenitors proliferate and differentiate. On day 33, retinal ganglion cells gradually were visible near the center of the retina, where *Brn3b* expression started to level up, turning on tdTomato expression, which sparsely distributed from the center to the edge of the organoid (Figure 2; white arrow).
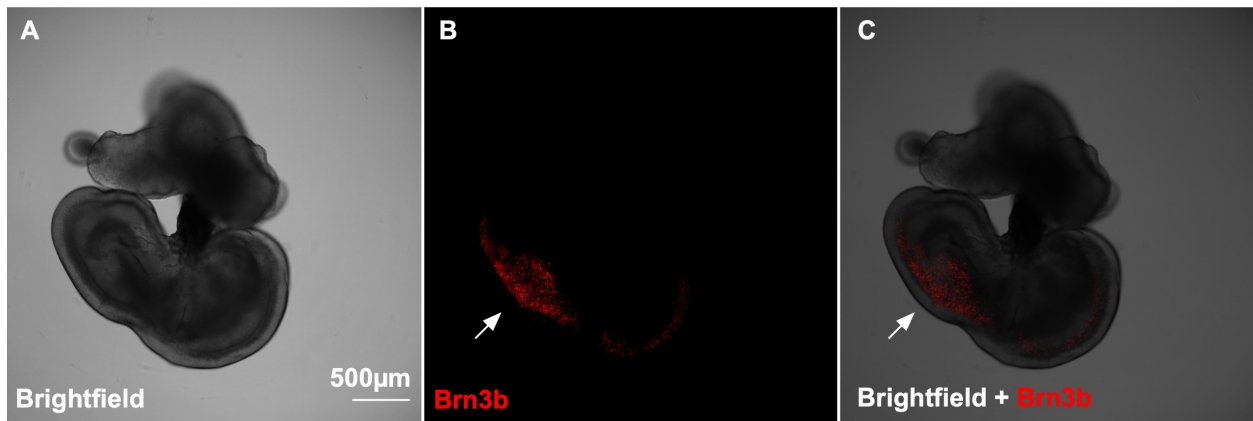
Figure 2. 4x Confocal imaging of d33 Brn3b-p2a-H2B-TdTOMATO / GLAST-p2a-H2B-eGFP IMR90.4-derived 3D retinal organoid. Arrow points early expression of Brn3b-driven TdTOMATO fluorescent protein indicating retinal ganglion cell nucleus location. Scale bar = 500µm.

The number of retinal ganglion cells kept rising as more and more of them were born from retinal progenitors and expanding the retinal ganglion cell layer, forming a lining of red nucleus with elevating *Brn3b* expression level reflecting in increasing tdTomato intensity from d40 (Figure 3). High number of retinal ganglion cells were generated from retinal progenitor cells from near center of the organoids, as their localization was shown by *Brn3b*-H2B-tdTomato marked nucleus.
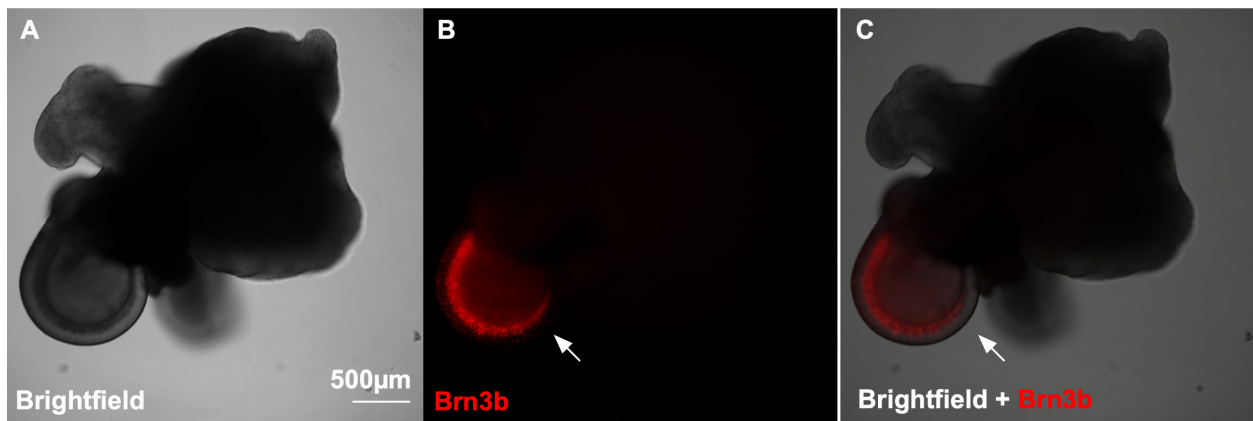


Figure 3. 4x Confocal imaging of d40 Brn3b H2B TOMATO GLAST H2B GFP IMR90.4-derived 3D retinal organoid. Arrow shows robust expression of Brn3b-driven TOMATO fluorescent protein indicating retinal ganglion cell nucleus location. Retinal ganglion cells are slowly migrating, forming a line at the edge of the retina. Scale bar = 500um.

On d50, *Brn3b* H2B tdTomato expression became very robust (Figure 4). Even though the changes in their distribution from d40 to d50 was subtle, retinal ganglion cells could be seen to widely spread across the immature sheet of neuroepithelium.
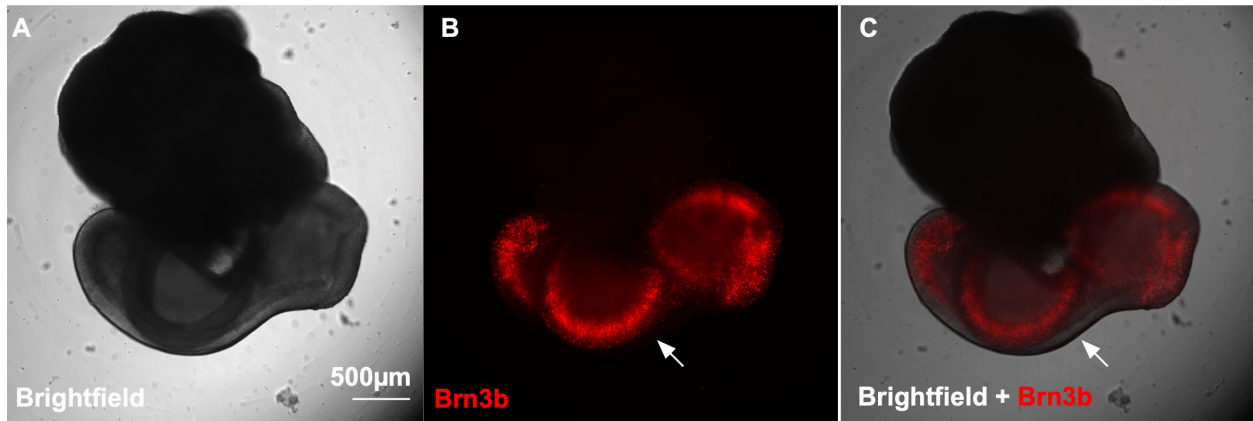


Figure 4. 4x Confocal imaging of d50 Brn3b H2B TOMATO GLAST H2B GFP IMR90.4-derived 3D retinal organoid. Arrow shows robust expression of Brn3b-driven TOMATO fluorescent protein indicating retinal ganglion cell nucleus location. Retinal ganglion cells are slowly migrating, forming a line at the edge of the retina. Scale bar = 500μm.

As the organoids maturated, retinal ganglion cells gradually formed a clear boarder between the center of the optic vesicle and the edges on d60 (Figure 5). However, *GLAST*-H2B-eGFP signals were still undetectable.
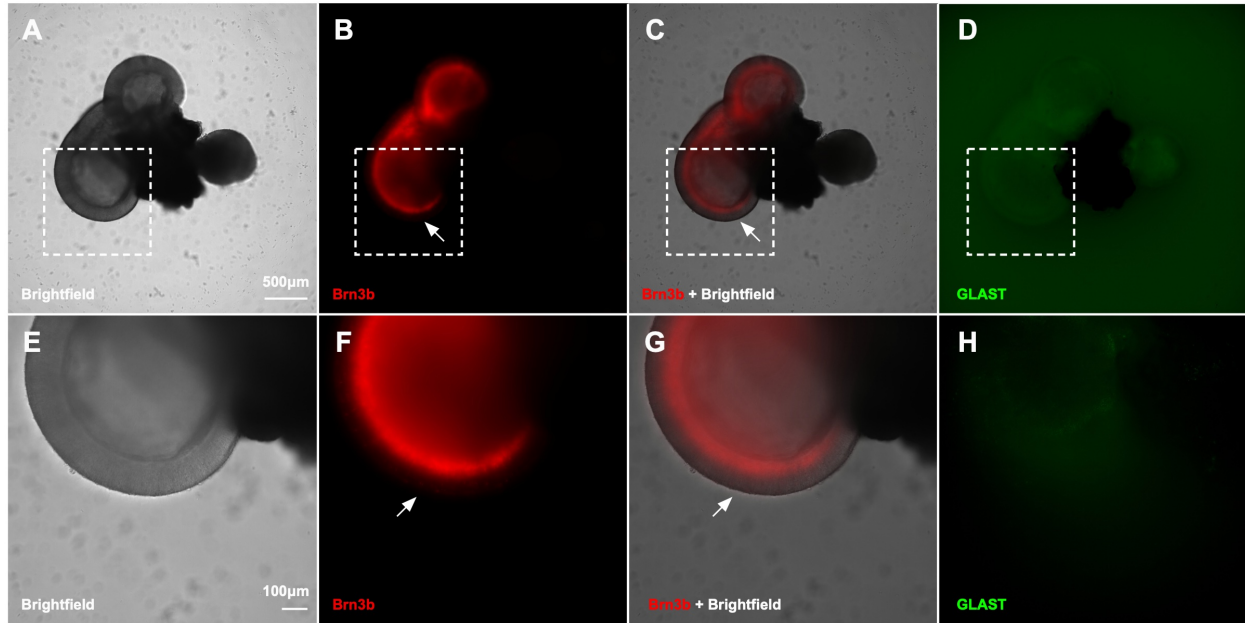
Figure 5. A-D. 4x Confocal imaging of d60 Brn3b H2B TOMATO GLAST H2B GFP IMR90.4-derived 3D retinal organoid. E-H. 10x Confocal imaging of d60 Brn3b H2B TOMATO GLAST H2B GFP IMR90.4-derived 3D retinal organoid. Arrow shows robust expression of Brn3b-driven TOMATO fluorescent protein indicating retinal ganglion cell nucleus location. Early sign of GLAST H2B GFP expression is shown in the center of retina, but at very low expression level. Retinal ganglion cells almost finished migrating and formed a line on the edge of the retina, shown by the arrow pointing. For A-D: Scale bar = $500\mu$m. For E-H: Scale bar = $100\mu$m.

On d70, the thickness of the retinal organoid continued to grow, while more retinal ganglion cells were generated, shown by the robust expression of *Brn3b*-H2B-tdTomato across the basal layer of the organoid (Figure 6). Over time, the non-retinal area of the organoid began to show weak green signals, but those were due to autofluorescence of dead cells at the center of the non-retinal structure due to lack of nutrient.
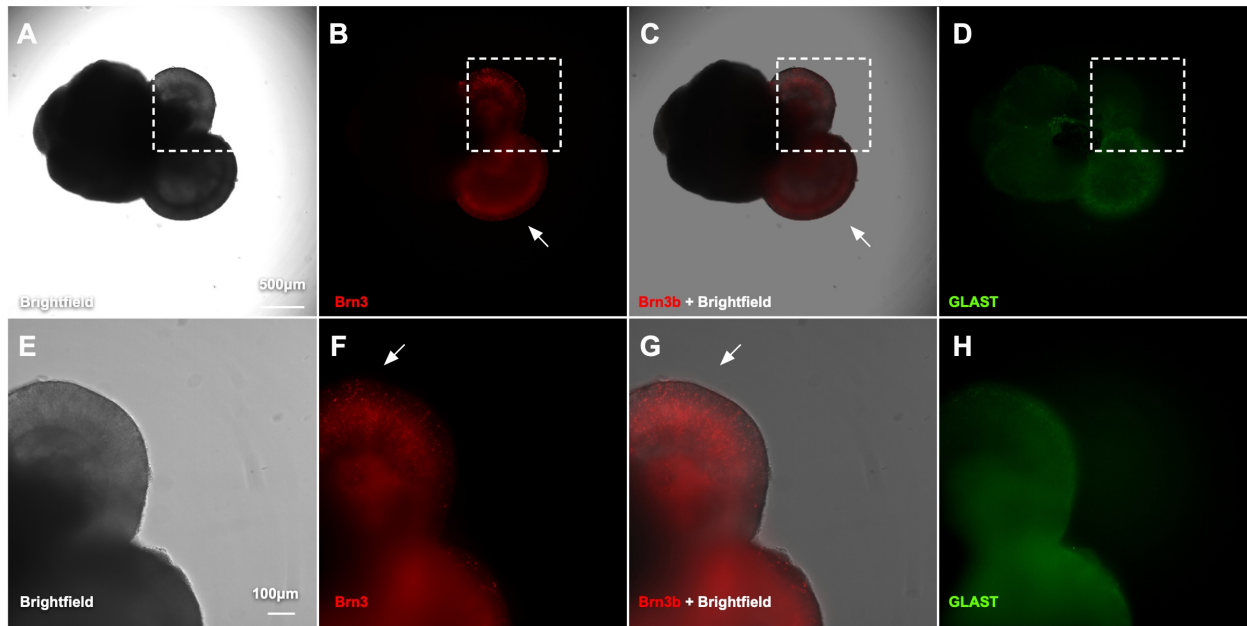
Figure 6. A-D. 4x Confocal imaging of d70 Brn3b H2B TOMATO GLAST H2B GFP IMR90.4-derived 3D retinal organoid. E-H. 10x Confocal imaging of d70 Brn3b H2B TOMATO GLAST H2B GFP IMR90.4-derived 3D retinal organoid. Arrow shows robust expression of Brn3b-driven TOMATO fluorescent protein indicating retinal ganglion cell nucleus location. Low level of GLAST-H2B-GFP expression can be seen in the center of retina. Retinal ganglion cells almost finished migrating and formed a line on the edge of the retina, shown by the arrow pointing. For A-D: Scale bar = $500\mu$m. For E-H: Scale bar = $100\mu$m.

As the retinal organoid progressed to d80, retinal ganglion cells continued to express high levels of *Brn3b* proteins aggregated along the basal side of the retina (Figure 7). However, some of these retinal ganglion cells have yet to finish migration, and their nucleus appeared to be migrating across the retina. *GLAST*-H2B-GFP at this point was still undetectable; the green pattern shown under 10X imaging was possibly false-positive signal emitted from the dead cells inside the non-retinal structure.
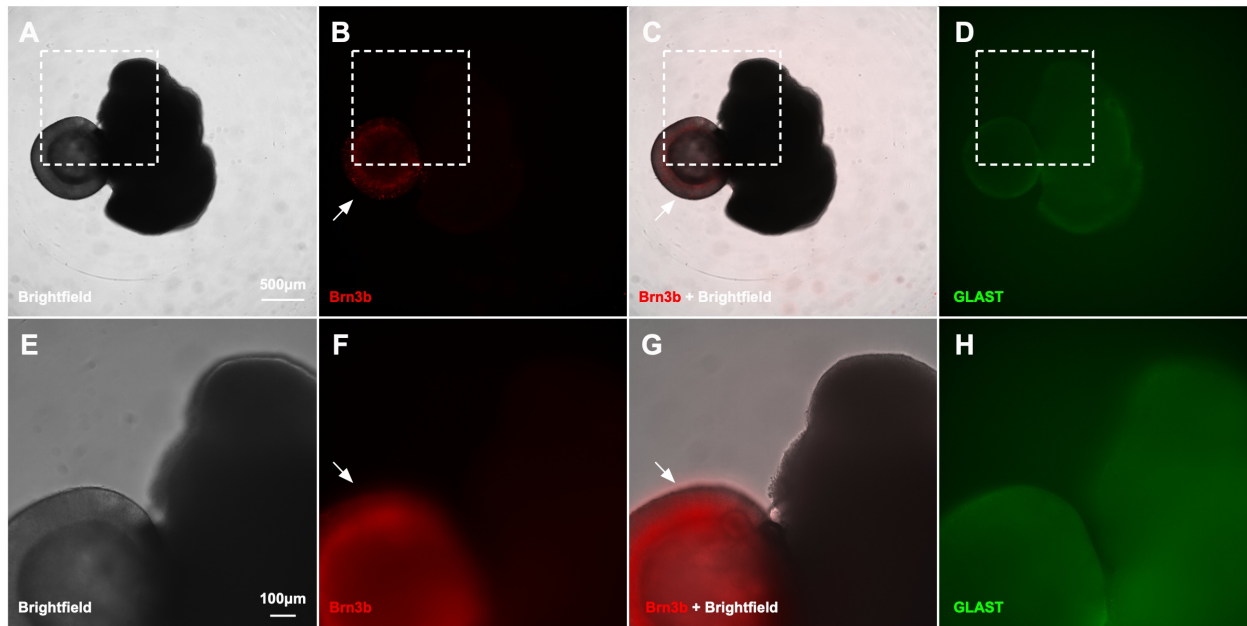
Figure 7. A-D. 4x Confocal imaging of d80 Brn3b H2B TOMATO GLAST H2B GFP IMR90.4-derived 3D retinal organoid. E-H. 10x Confocal imaging of d80 Brn3b H2B TOMATO GLAST H2B GFP IMR90.4-derived 3D retinal organoid. Arrow shows robust expression of Brn3b-driven TOMATO fluorescent protein indicating retinal ganglion cell nucleus location. GLAST H2B GFP expression level remained low at this stage. Retinal ganglion cells almost finished migrating and formed a line on the edge of the retina, shown by the arrow pointing. For A-D: Scale bar = 500$\mu$m. For E-H: Scale bar = 100$\mu$m.

On d90, a retinal ganglion cell layer continued to be apparent, and appeared to form a more compacted *Brn3b*-H2B-tdTomato region as compared to earlier time points which appeared to have more cells in transit (Figure 6). At this stage, few of these *Brn3b*-H2B-tdTomato positive nuclei could be detected at the margin of the outer layer of the organoid, while most of them presented their existence accumulating along the inner surface of the neuroepithelium. Weak expression of *GLAST*-H2B-GFP emerged from the center of the retinal organoid and slowly migrate toward the edges (Figure 8; Green arrow).
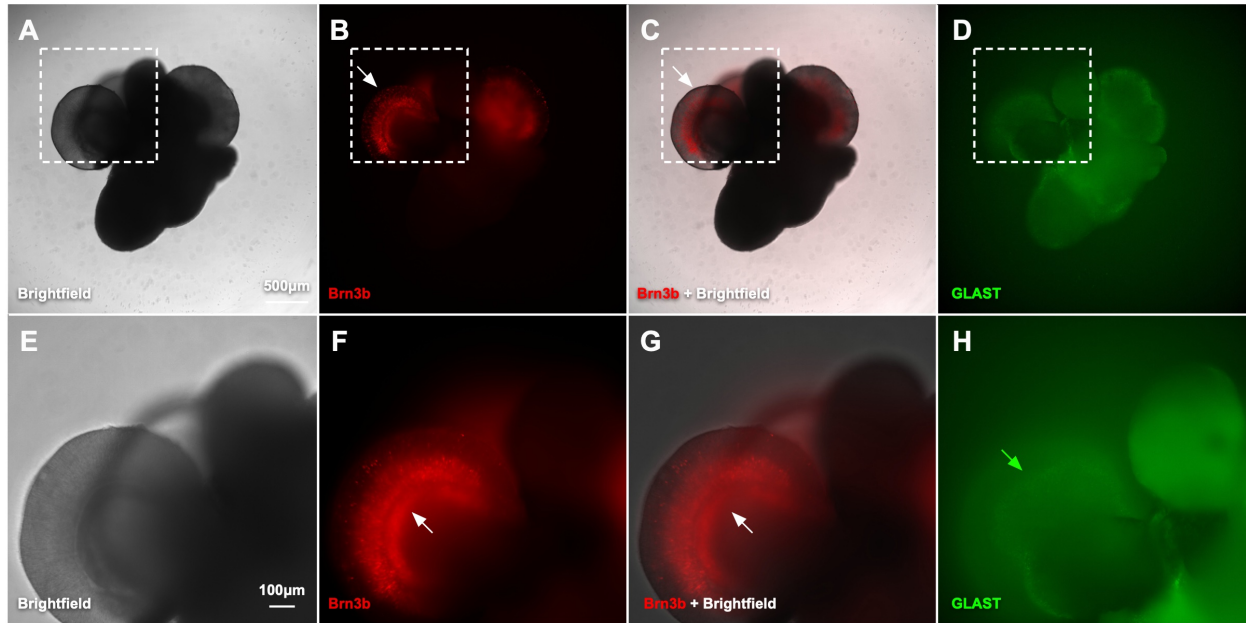
Figure 8. A-D. 4x Confocal imaging of d90 Brn3b H2B TOMATO GLAST H2B GFP IMR90.4-derived 3D retinal organoid. E-H. 10x Confocal imaging of d90 Brn3b H2B TOMATO GLAST H2B GFP IMR90.4-derived 3D retinal organoid. Arrow shows robust expression of Brn3b-driven TOMATO fluorescent protein indicating retinal ganglion cell nucleus location. Early sign of GLAST H2B GFP expression is shown in the center of retina, but at very low expression level. Retinal ganglion cells had finished migrating and formed a line on the edge of the retina, shown by the white arrow pointing. Weak GLAST-H2B-GFP signal could be detected originating from the center of the retina, as shown by the green arrow pointing in pannel (H). For A-D: Scale bar = 500$\mu$m. For E-H: Scale bar = 100$\mu$m.

To better visualize the expression of dual reporters, organoids were collected at days 60, 70, 80 and 90 and cryosectioned at a thickness of 10μm. Tissue sections were cover slipped facing downwards and imaged using with a high quality camera attached to a Leica fluorescence microscope. The captured raw images were processed using ImageJ. At d60, *Brn3b*-H2B-tdTomato expression pattern indicated that the retinal ganglion cells were sparsely spread across the layers of retinal organoids, and *GLAST*-H2B-GFP in Müller cells had not yet accumulated to a level that can be visualized by fluorescent microscope (Figure 9).
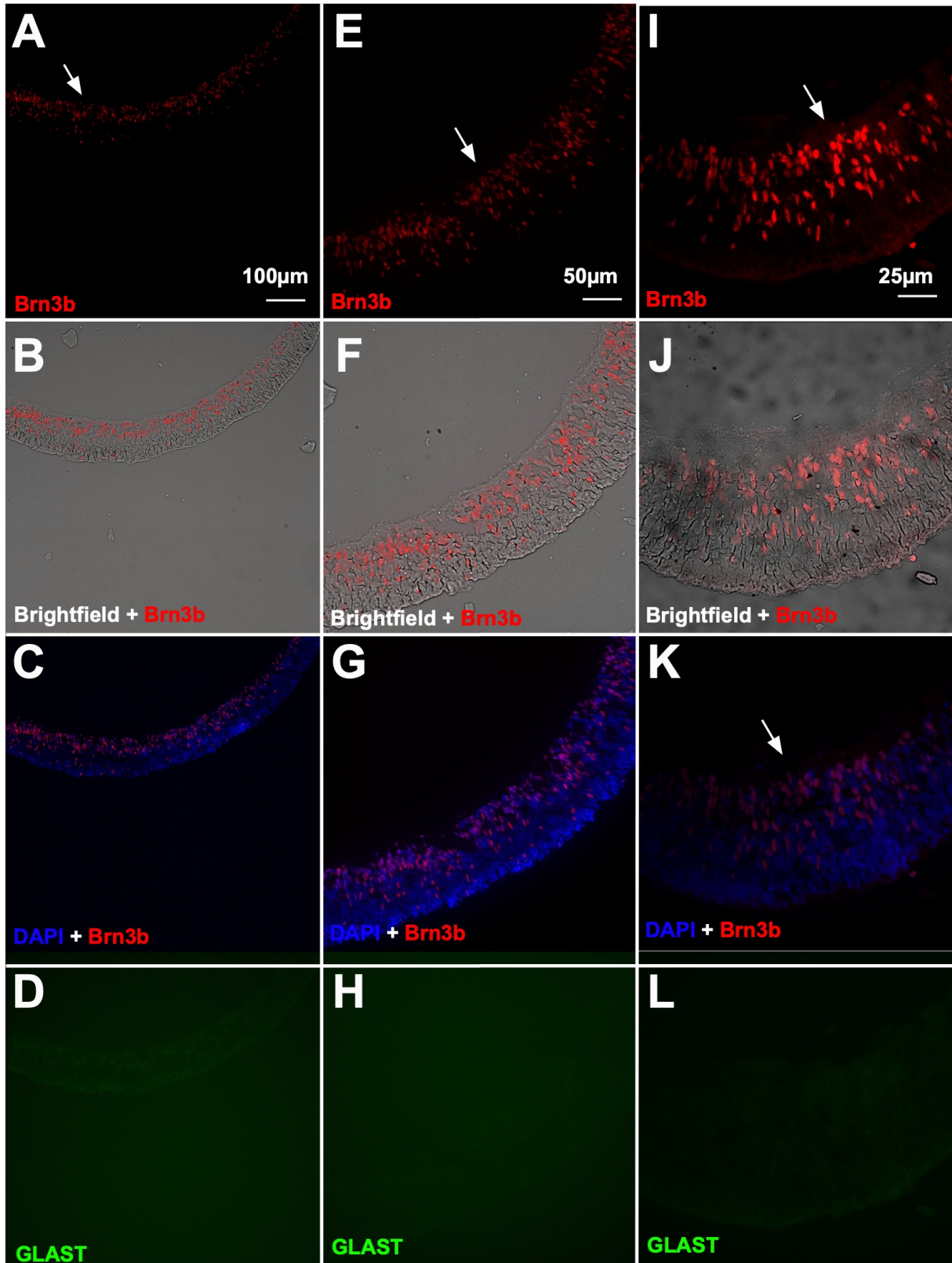
Figure 9. 10x (A-D), 20x (E-H) and 40x (I-L) Confocal imaging of cryosectioned d60 Brn3b H2B TOMATO GLAST H2B GFP IMR90.4-derived 3D retinal organoid. White arrows point to the lining of Brn3b-H2B-tdTomato positive retinal ganglion cell nucleus. For A-D: Scale bar = 100$\mu$m. For E-H: Scale bar = 50$\mu$m. For I-L: Scale bar = 25$\mu$m.

Hence there is no guarantee to prove Müller cell existence on d60. As the organoid continued to develop, on d70 and d80, the retinal ganglion cells migrated closer and closer toward each other, even though some of them still linger across layers of the retinal organoid, large proportion of retinal ganglion cells began to line up (Figure 10-11).
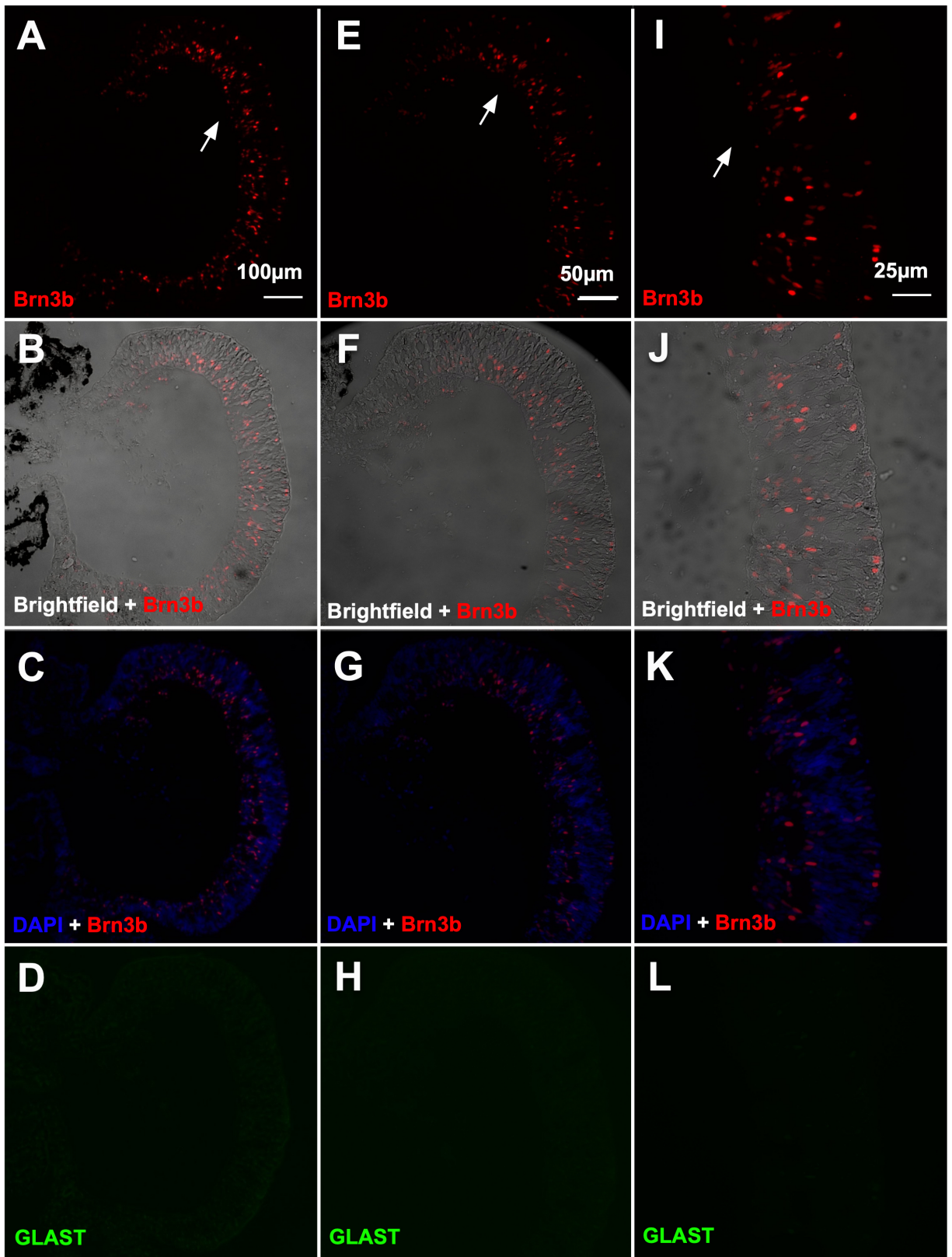
Figure 10. 10x (A-D), 20x (E-H) and 40x (I-L) Confocal imaging of cryosectioned d70 Brn3b H2B TOMATO GLAST H2B GFP IMR90.4-derived 3D retinal organoid. White arrows point to the lining of Brn3b-H2B-tdTomato positive retinal ganglion cell nucleus. For A-D: Scale bar = 100$\mu$m. For E-H: Scale bar = 50$\mu$m. For I-L: Scale bar = 25$\mu$m.

26

Figure 11. 10x (A-D), 20x (E-H) and 40x (I-L) Confocal imaging of cryosectioned d80 Brn3b H2B TOMATO GLAST H2B GFP IMR90.4-derived 3D retinal organoid. White arrows point to the lining of Brn3b-H2B-tdTomato positive retinal ganglion cell nucleus. For A-F: Scale bar = 100$\mu$m. For E-H: Scale bar = 50$\mu$m. For I-L: Scale bar = 25$\mu$m.

27

It was not until d90 that a compact retinal ganglion cell layer has formed, as the outer

layer of retinal organoid grew thicker and thicker, and an early weak expression of *GLAST*-H2B-

GFP started to emerge from the center of the organoid where the retinal progenitor cells are
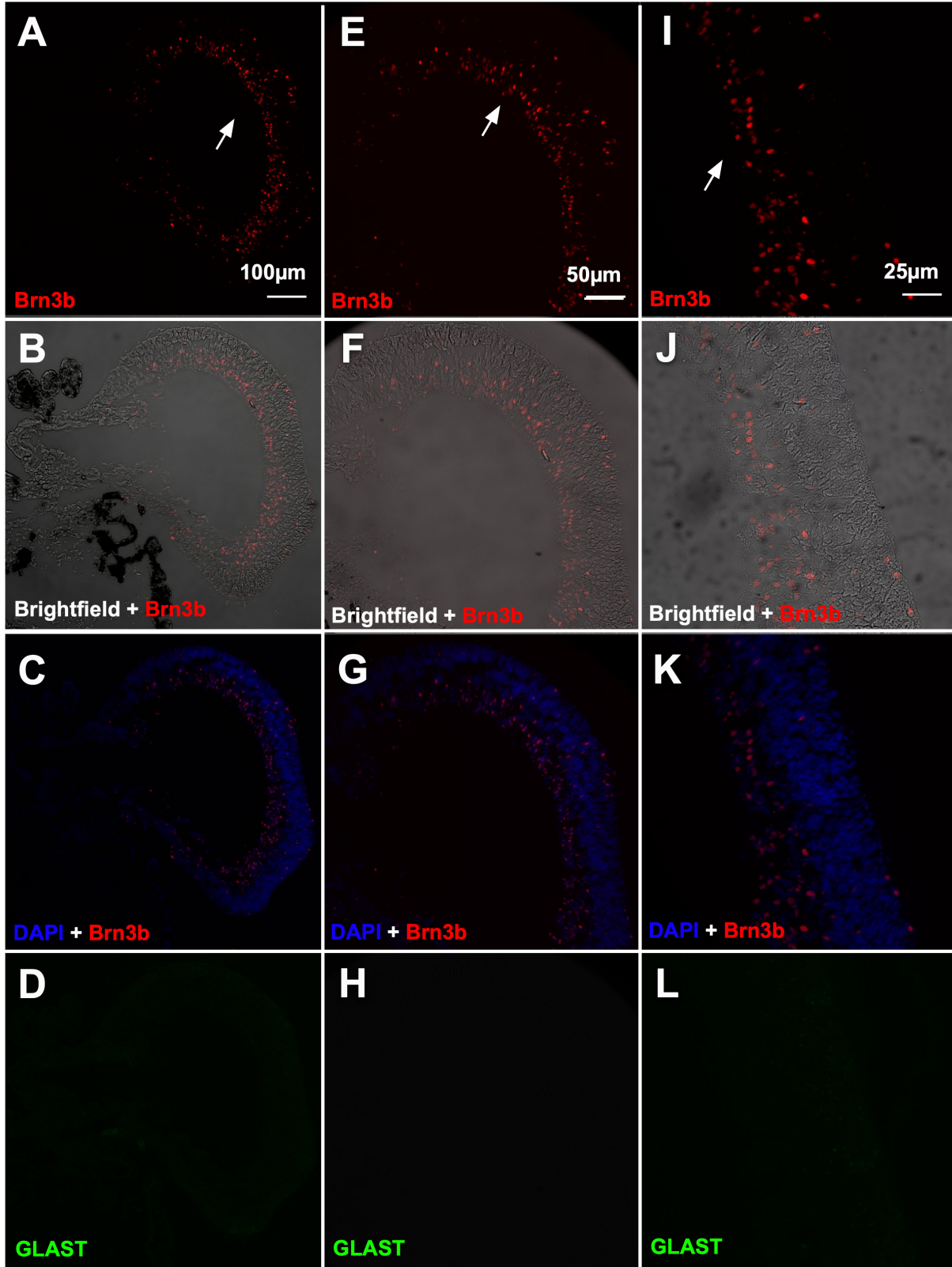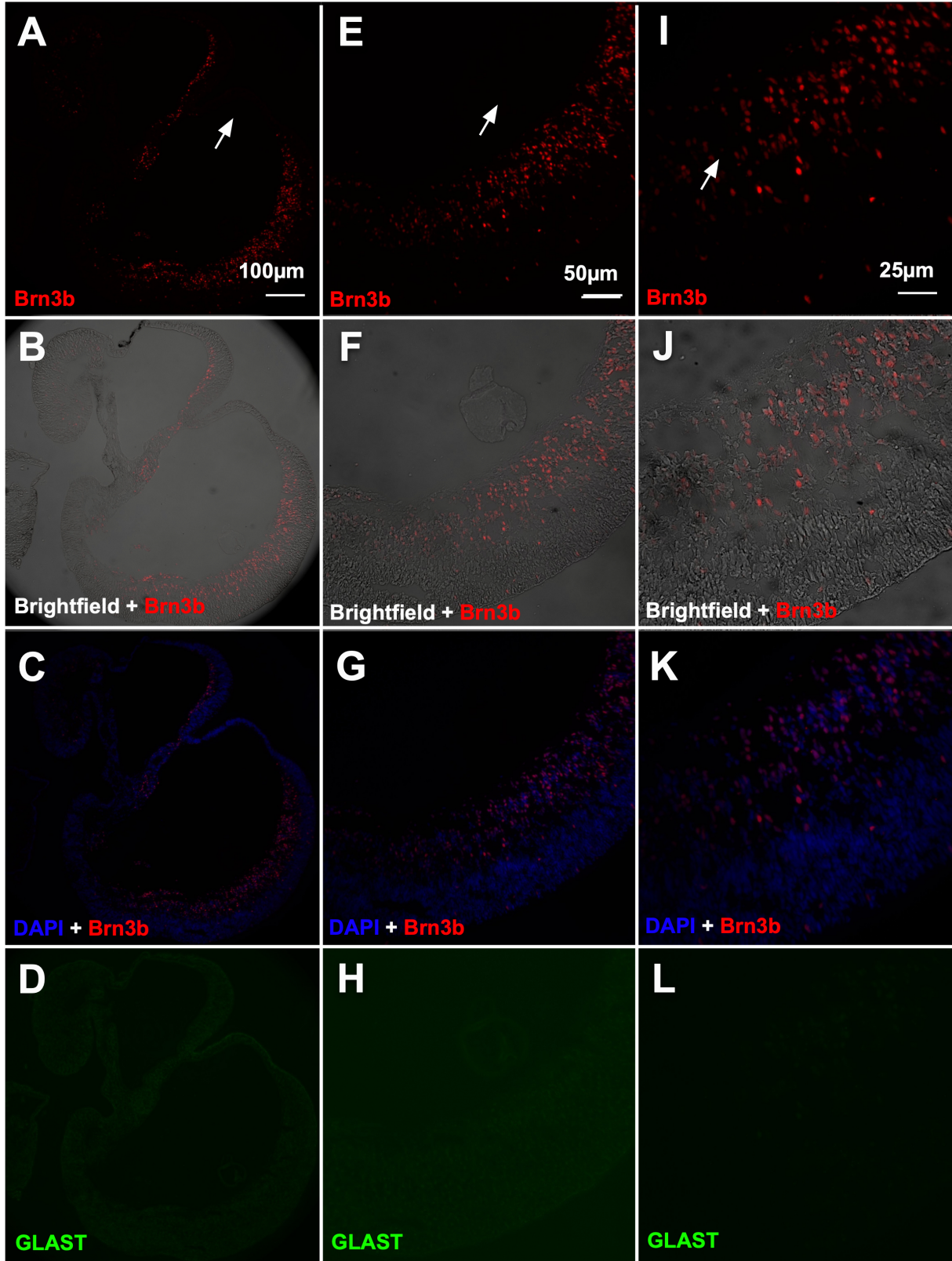
located (Figure 12)

Figure 12. 10x (A-D), 20x (E-H) and 40x (I-L) Confocal imaging of cryosectioned d90 Brn3b H2B TOMATO GLAST H2B GFP IMR90.4-derived 3D retinal organoid. White arrows point to the lining of Brn3b-H2B-tdTomato positive retinal ganglion cell nucleus. For A-D: Scale bar = 100$\mu$m. For E-H: Scale bar = 50$\mu$m. For I-L: Scale bar = 25$\mu$m.

29

Although *GLAST*-H2B-GFP expression in Müller Glia in retina occurred later than expected, its expression in non-retinal organoid was much earlier and far more robust comparing to that in retinal organoid(Figure 13).
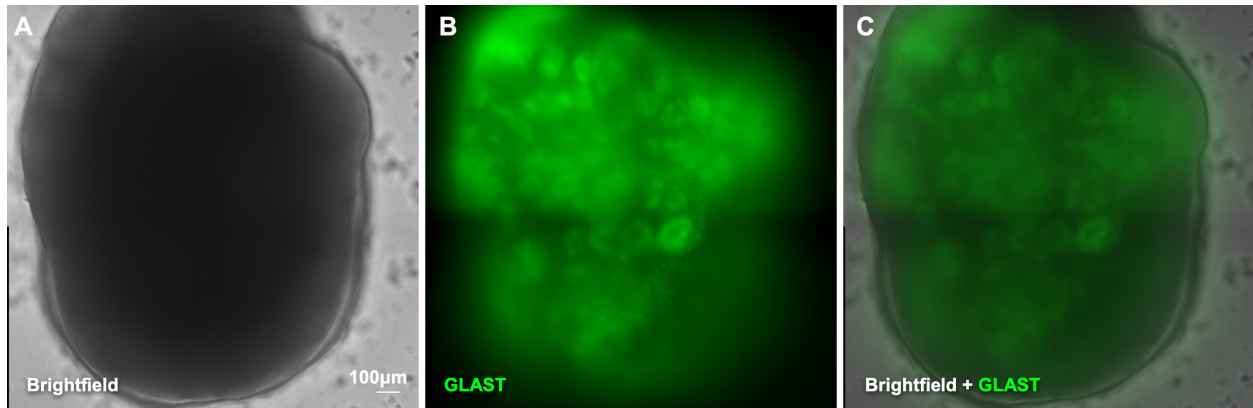


Figure 13. 10x live cell imaging of d50 GLAST H2B GFP IMR90.4-derived 3D non-retinal organoid. Scale bar = 100$\mu$m.

To better visualize the *GLAST*-driven EGFP expression, the non-retinal organoids were then dissociated and plated on matrigel coated cell culture plates. The 2D cultures of dissociated non-retinal organoids displayed high levels of *GLAST-2a-H2B*-GFP expression after several weeks later when the cells became extremely high density culture (Figure 14; white arrow). If the dissociated culture were not as compacted, the *GLAST*-H2B-GFP would not be expressed (Figure 14, yellow arrow).
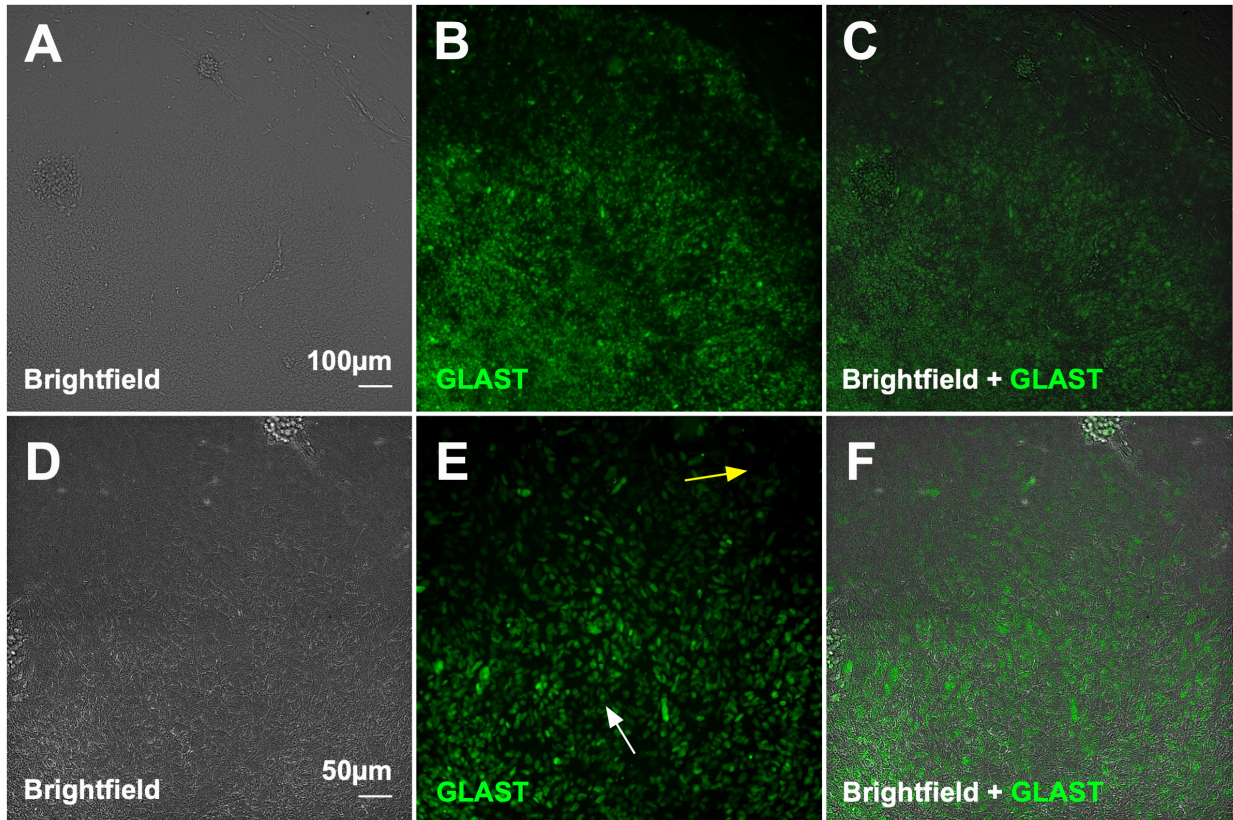
Figure 14. 10x (A-F) and 20x (G-I) live cell imaging of Glial cells grown in 2D from d70+70 dissociated Brn3b-p2a-H2B-TOMATO / GLAST-p2a-H2B-eGFP IMR90.4 iPSC derived non-retinal organoids. GLAST H2B GFP expression level is higher at compacted areas (white arrow) than sparse area (yellow arrow). For A-C: Scale bar = 100$\mu$m. For D-F: Scale bar = 50$\mu$m.

To further confirm the presence of Müller Glia in 2D dissociated non-retinal organoid cultures, cells were collected for mRNA extraction. The extracted mRNA was reverse-transcribed into cDNA and PCR amplified for detection of the Müller cell and astrocyte specific markers (*SLC1A3*, *GLUL* and *GFAP*) along with the house keeping gene and the retinal ganglion cell specific marker, *Brn3b*. The agarose gel electrophoresis result reflected high level of *GFAP* mRNA expression moderate level of *SLC1A3* expression, and weak level of *GLUL* mRNA expression, all of which pointed to the mass amount of astrocytes in non-retinal organoid (Figure 15). The primer binding for *Brn3b* was not specific, and none of those two bands were the correct product size that points to *Brn3b* presence.
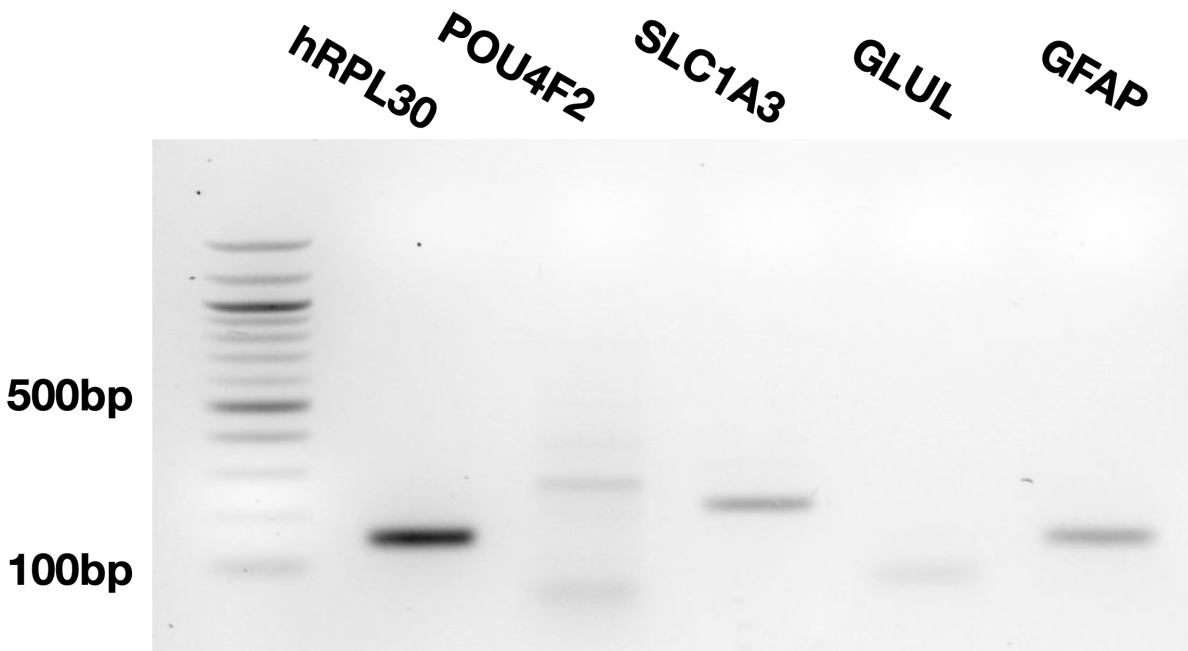
Figure 15. Agarose gel electrophoresis of PCR products from cDNA reverse-transcribed from mRNA extracted from d50+70 GLAST H2B GFP IMR90.4 derived 3D non-retinal organoid to detect astrocyte markers: GLAST, GLUL and GFAP.

The pattern of mRNA expression level in d90 *Brn3b* H2B tdTomato *GLAST* H2B GFP IMR90.4 retinal organoid was similar to that in the non-retinal organoid despite *GLUL* level was too low to be detected (Figure 16). Since the retinal organoids did not have vascularization, it is not possible for retinal astrocytes to form in the 3D organoids grew in this experiment (Vecino et al., 2016). Hence the presence of Müller cell in retinal organoid on d90 was confirmed. The d90 *Brn3b* H2B tdTomato *GLAST* H2B GFP IMR90.4 retinal organoid did not show positive for *Brn3b* mRNA even though high levels of *Brn3b*-H2B-tdTomato was visualized under fluorescent scope. Hence, similar to what happened in the experiment with non-retinal organoid mentioned above, the primer set used to detect *Brn3b* mRNA in d90 *Brn3b* H2B tdTomato *GLAST* H2B GFP IMR90.4 retinal organoid did not proven to be sufficient for correct *Brn3b* presence indication.
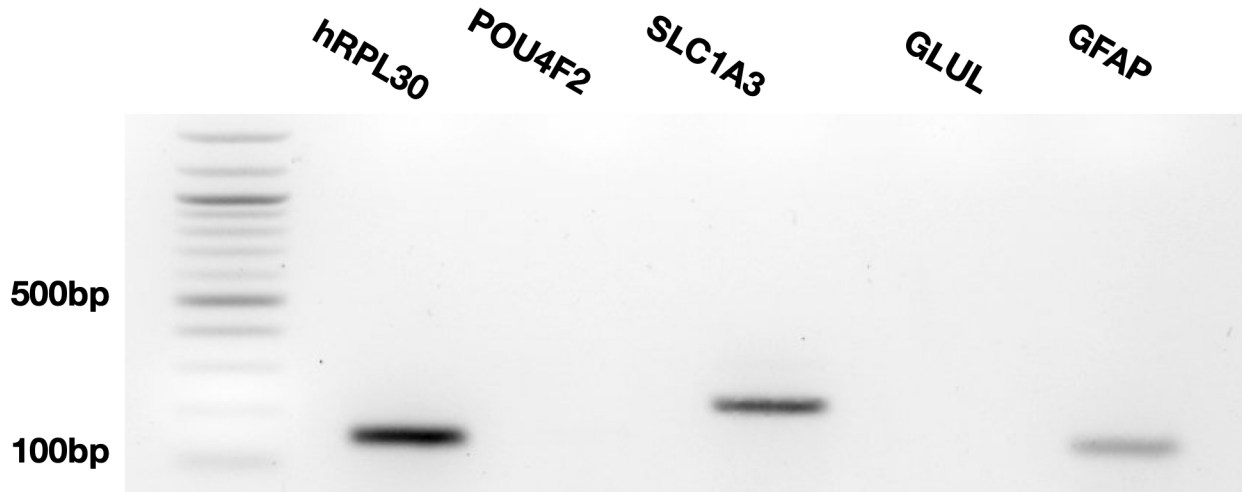
Figure 16. Agarose gel electrophoresis of PCR products from cDNA reverse-transcribed from d90 Brn3b H2B tdTomato GLAST H2B GFP IMR90.4 derived 3D retinal organoid to detect astrocyte markers: GLAST, GLUL and GFAP.

On the other hand, GLAST is expressed at a very low level in iPSC stage also. The level is so low that GLAST-H2B-GFP reporter could not be seen but a lineage tracing system did reveal this unexpected finding. Right after transfecting the lineage trace system into iPSCs, many cells acquired red fluorescence as they were expanding(Figure 18). To investigate whether this phenomenon was due to dysfunctional STOP site leading to leakage expression or CRE mediated excision actually happened, the transfected cell line genome was extracted, PCR amplified and sent for sequencing. The primers used for amplifying target strand flanked LOXP STOP LOXP site (Schematic 6).
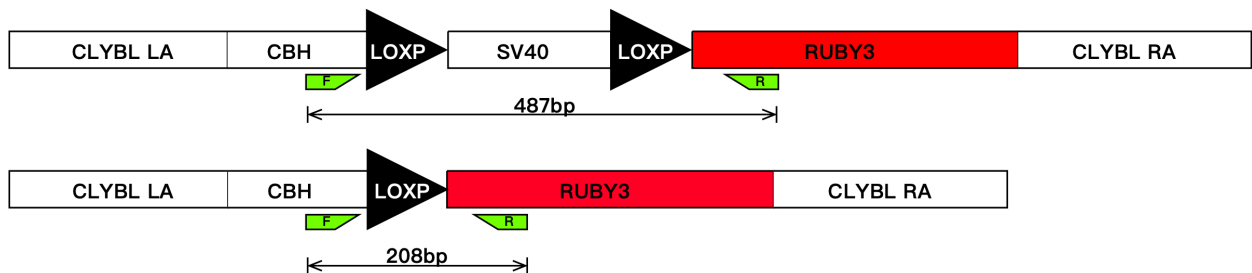


Schematic 6. Sequencing range between primer binding sites to confirm 10x image of 2D culture of GLAST NLS CRE CLYBL LOXP STOP LOXP CBH RUBY3 Brn3b H2B GFP iPSC cell line.

After CRE recombinase was expressed, one of the LoxP sequence and a STOP site should

be cleaved, and a shorter band can be seen on the gel (Figure 17).
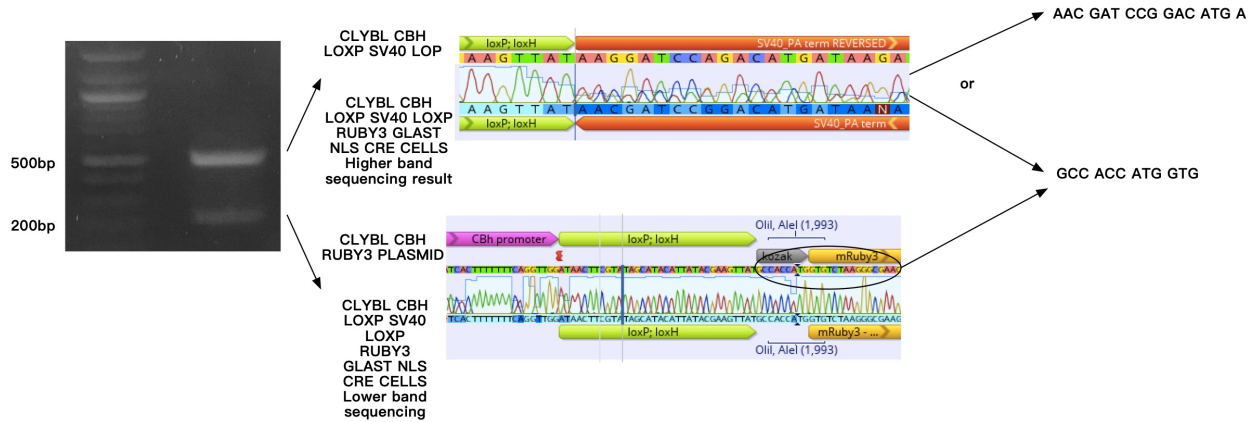


Figure 17. Sequencing result confirming CRE cleavage comparing to designed plasmid map.

Two bands with different sizes shown on the gel were sent in for sequencing. The higher

band was a mixture of uncleaved LOXP STOP LOXP and cleaved LOXP RUBY3 sequence

while the lower band reads only cleaved LOXP RUBY3 sequence, showing successful cleavage

(Figure 17). The cleaved sequence presented on both top and bottom because some colonies were

heterozygous at which only one of the alleles were successfully recognized by CRE recombinase

and cleaved.
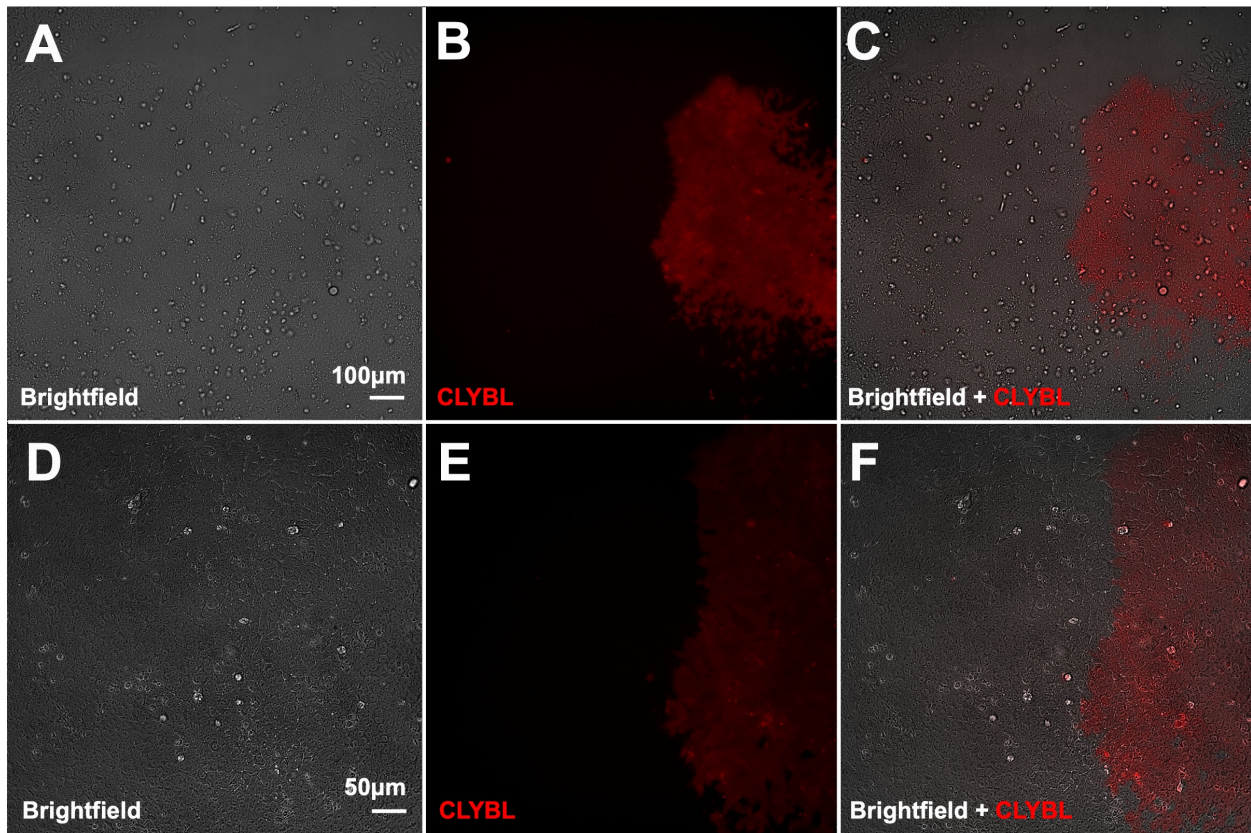
Figure 18. 10x (A-C) and 20x (D-F) image of 2D mixed population of GLAST NLS CRE CLYBL LOXP STOP LOXP CBH RUBY3 Brn3b H2B GFP IMR90.4 iPSC cell line. Only part of the population is positive for Ruby3 fluorescent protein expression. For A-C: Scale bar = $100\mu$m. For D-F: Scale bar = $50\mu$m.

After cleavage, *CLYBL* driven Ruby3 was expressed not only at stem cell stage, but also in differentiating organoid as well (Figure 19 to 21). However, as the differentiation stage progresses, the expression level of *CLYBL* was slowly turning down. This pattern was verified in the lab in an RNAseq dataset (data not shown).

Figure 19. Ruby3 positive d5 organoid differentiated from GLAST NLS CRE CLYBL LOXP STOP LOXP CBH RUBY3 Brn3b H2B GFP IMR90.4 iPSC cell line. Scale bar = 100$\mu$m.



Figure 20. Ruby3 positive d10 organoid differentiated from GLAST NLS CRE CLYBL LOXP STOP LOXP CBH RUBY3 Brn3b H2B GFP IMR90.4 iPSC cell line. Scale bar = 100$\mu$m.



Figure 21. Ruby3 positive d20 organoid differentiated from GLAST NLS CRE CLYBL LOXP STOP LOXP CBH RUBY3 Brn3b H2B GFP IMR90.4 iPSC cell line. Scale bar = 100$\mu$m.

*CLYBL* Ruby3 intensity was gradually epigenetically silenced while Brn3b expression

turned on as usual on d30, displaying that *CLYBL* safe harbor sites still needs further

developments (Figure 22).
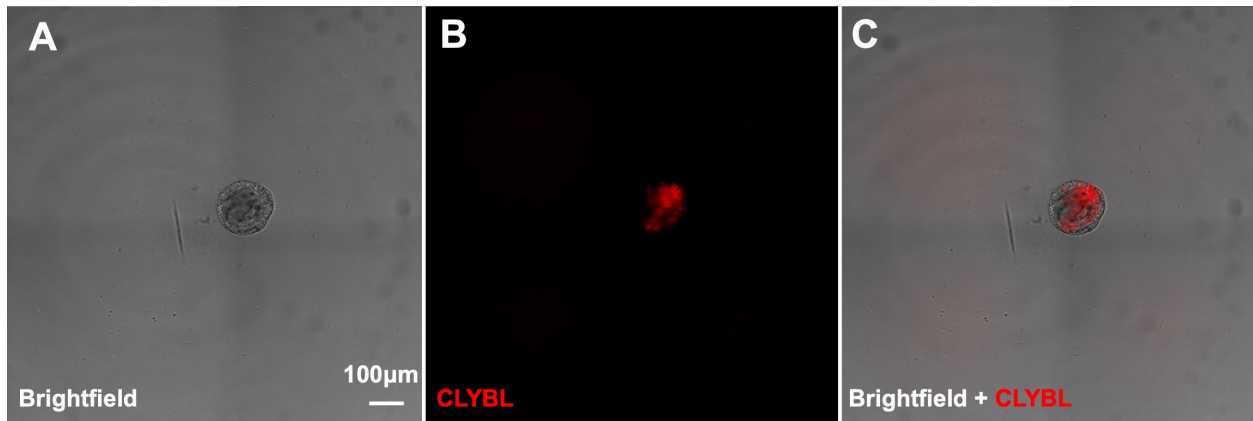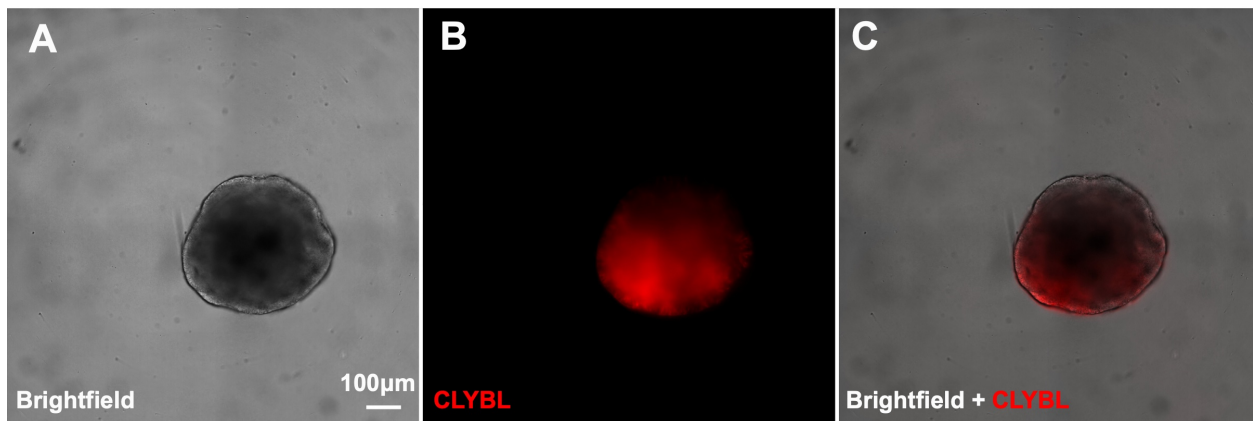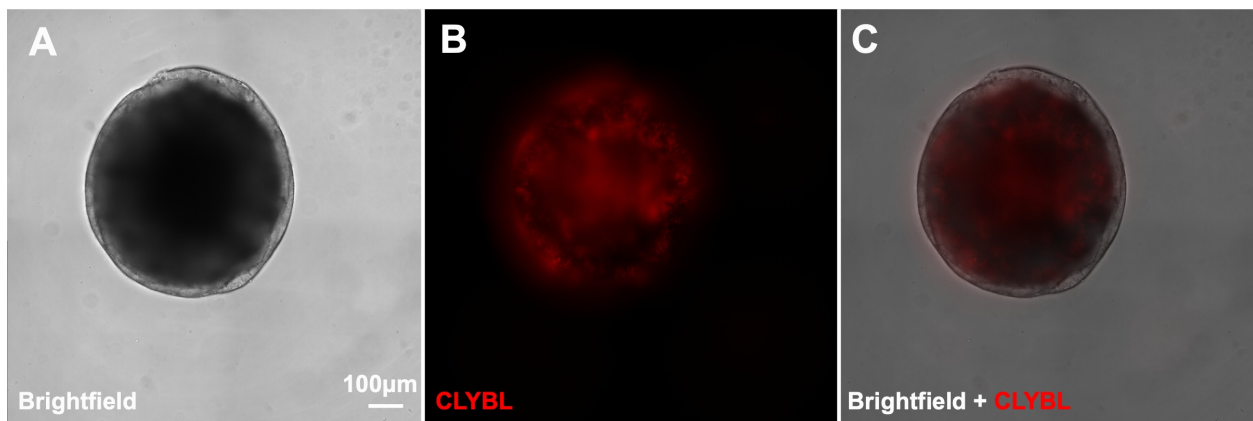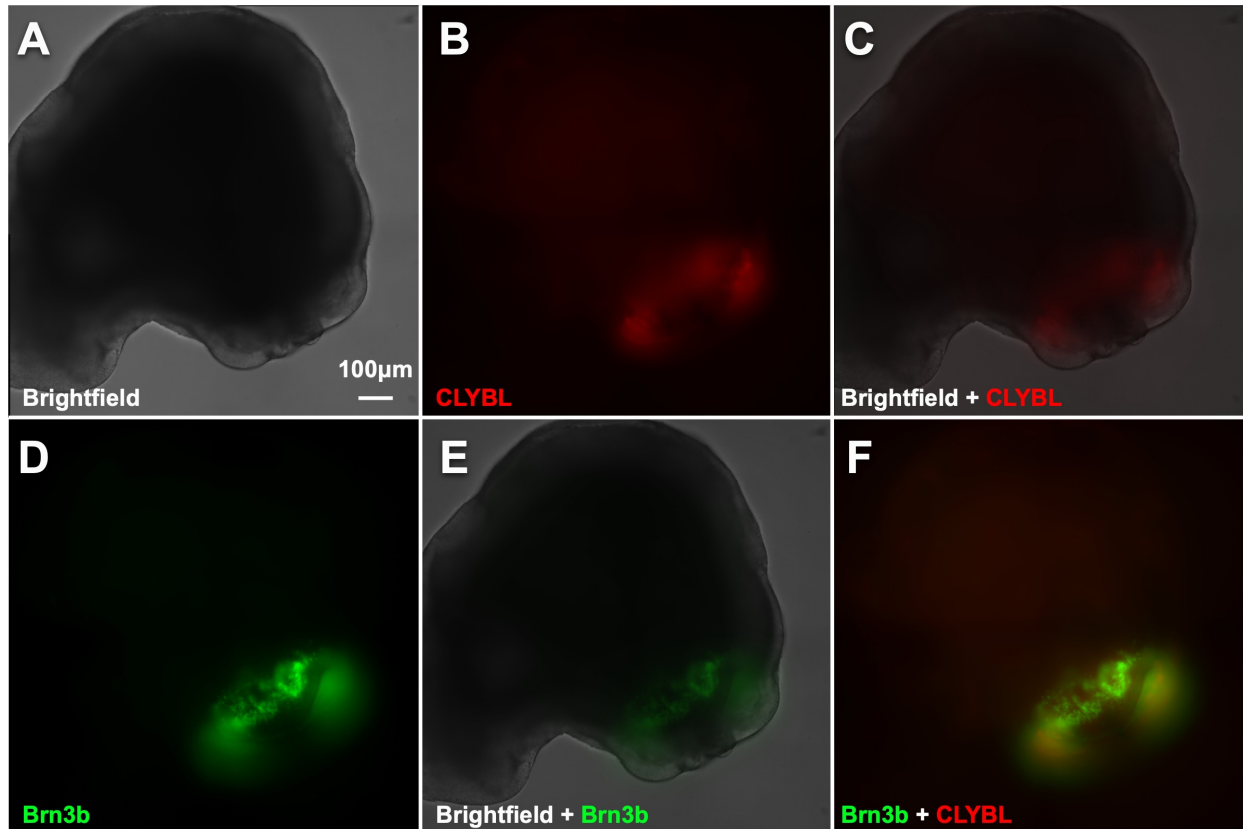


Figure 22. Ruby3 positive d30 organoid differentiated from GLAST NLS CRE CLYBL LOXP STOP LOXP CBH RUBY3 Brn3b H2B GFP iPSC cell line. Brn3b-H2B-GFP started to show at this time. Scale bar = $100\mu$m.

Discussion

In this study, a dual reporter was successfully built, which was able to detect glial cells in developing retina and non-retinal structure. Even though *GLAST* expression level turned out to be much lower than expected and did not reach high peak until later than expected experiment period. Considering Müller Glia only consists of less than 5% of retinal cells (Fischer, 2011), it is possible that *GLAST* expression inside Müller Glia is too low to be visualized either by eye or under fluorescent scope. However, *GLAST* is highly expressed in brain as a major transporter for removal of neurotransmitter glutamate (Zhou and Danbolt, 2013). The dissociated 2D culture from non-retinal organoids displayed robust and constitutive *GLAST*-H2B-GFP expression, which is further confirmed by PCR amplification of cDNA reverse-transcribed from mRNA extracted from *GLAST*-H2B-eGFP positive 2D culture, indicating glial cell existence. This density-related GLAST expression level clearly requires more in-depth study.

Even though d90 *Brn3b* H2B tdTomato *GLAST* H2B GFP retinal organoids failed to display strong *GLAST* driven GFP expression, the mRNA expression level clearly pointed to early sign of Müller glia generation. One phenomenon discovered during the experiment using lineage tracing system was *GLAST* expression pattern in stem cell stage, which was not previously reported in other studies. This discovery can be used to study the function of GLAST at stem cell stage and its interaction with other genomic pathways. On the other hand, partially verified that Lineage Trace System can be used in differentiating retina that will aid in future endogenous regeneration studies.

The next step for this study is to extend the period of dual reporter system study until genuine *GLAST*-H2B-eGFP expression can be seen. Also, other Müller cell markers should be used to drive CRE recombinase in the Lineage trace system, which can then be used in the

Endogenous Regeneration project, which focuses on activating Müller Glia's regenerative potential to restore photoreceptors and retinal ganglion cells but also has an indicator in those regenerated cells to prove Müller cell origin.

Material and Methods

**Plasmid design and construction: MC *Brn3b* tdTomato H2B and MC *Brn3b* Neon H2B.** The MC *Brn3b* H2B tdTomato and MC *Brn3b* Neon H2B vector was constructed by inserting a H2B nucleus marker to tag the tdTomato or Neon fluorescent protein coding sequence cassette in between homology arms flanking 3' end of *Brn3b* coding sequences. P2A coding sequence was placed after fluorescent reporter cassette. *Brn3b* homology arms were cloned from genome extracted from human pluripotent stem cell line IMR90-4.

**Plasmid design and construction: *GLAST* H2B EGFP.** MC *GLAST* H2B GFP plasmid was constructed by inserting a H2B nucleus marker to tag the enhanced GFP fluorescent protein coding sequence cassette in between homology arms flanking 3' end of *GLAST* coding sequences. P2A coding sequence was placed after fluorescent reporter cassette. *GLAST* homology arms were cloned from genome extracted from human pluripotent stem cell line IMR90-4.

**Plasmid design and construction: Lineage tracing system.** NLS CRE fragment was amplified from pCAG-CRE-GFP plasmid, and then inserted into MC-*GLAST*-gRNA plasmid using NEB builder HIFI DNA assembly mastermix (NEB E2621S). The LoxP-STOP-LoxP cassette was constructed by cloning SV40-PA sequence from *AAVS1* Neo M2rttA plasmid (Addgene 60843) with oligo that have LoxP overhang. Then the whole LoxP-STOP-LoxP cassette was sub-cloned into *CLYBL*-CBH-Ruby3 plasmid.

**Induced human pluripotent stem cell line maintainence.** Induced human pluripotent stem cell lines H9 and IMR90.4 were maintained in mTESR1 (STEMCELL Technologies) on Matrigel Mix (Corning) coated 12-well tissue culture treated plates (USA Scientific). Upon passaging, these cells were dissociated by digesting cell culture with 0.5ml of Accutase (Sigma-

Aldrich) in each well of a 12-well tissue culture treated plates for 5 minutes in 37°C. The floating

cells were then quenched by adding 1ml of mTESR1 plus Blebbistatin (Sigma-Aldrich) in each

well of a 12-well tissue culture treated plates. The cells were collected and spun down at 80xg

for 5 minutes. The supernatant was removed and cell pellet was resuspended in fresh mTESR1

plus Blebbistatin. The cells were then plated at 1000 cells/well in 1ml of mTESR1 plus

Blebbistatin in each well of a 12-well tissue culture treated plates.

**Transfection of PSC by electroporation.** The dual reporter plasmids (MC *Brn3b* H2B

tdTomato P2A and MC *GLAST* H2B eGFP P2A) were transfected into IMR90.4 cells and the

lineage tracing plasmids mentioned above (MC-*GLAST*-NLS-CRE-gRNA and MC-*CLYBL*-

LOXP-STOP-LOXP-CBH-Ruby3) were transfected into H9 cells already harboring a *Brn3b*-

H2B-Neon tag using the Neon Transfection System (Thermo Fisher). Tet-inducible Cas9

harboring H9 *Brn3b*-H2B-Neon cells and IMR90.4 cells were treated with doxycycline 1 day

before and after transfection to maintain high levels of Cas9 for gene-editing. Briefly, 100,000 –

200,000 iPSC cells were incubated in 1ml of Accutase for 12 min at 37°C in hypoxia (5% O2,

10%CO2) before being collected and washed with 1ml of mTESR1 (STEM CELL technologies)

media with 5μM Blebbistatin (Sigma-Aldrich). The cells were then incubated on ice for 15

minutes before resuspension in plasmid containing R buffer plus DNA and electroporated in E

buffer at 1300V for 20ms. The electroporated cells were slowly added to 1ml recovery media

while circling pipette tip up and down and incubated in hood for 30 min to allow cells to settle to

bottom of tube. 0.5mL of cells from bottom of recovery tube were plated onto matrigel-coated 12

well TC treated plate.

**Differentiation of iPSC cells.** The transfected iPSC cells were passaged in 0.5 mL of accutase per well of a 12-well tissue culture treated plate and incubated at 37C for 5 mins and then gently triturated with P1000 tips 3 times before transferred to 2 mL of mTeSR1 plus Blebbistatin (5 µM). 125 cells were added in 50 µL mTeSR plus Blebbistatin into each well of a non-adherent round bottom 96-well plate. Cells were settled by gravity and put into hypoxic (5% $CO_2$, 10% $O_2$) incubator. The next day cells were fed with 50 µL BE6.2 media consisted of 10mL of E6 (homemade), 5mL of B27 without Vitamin A (ThermoFischer), 2.5mL of Glutamax 100X (Gibco), 2.5mL of NEAA 100X (Gibco), 2.5mL of Sodium Pyruvate 100X (Gibco) and use DMEM high glucose (Gibco) to bring to 250mL plus 2% matrigel plus 3µM of IWR-1e in each well. On day 2 and day 3, cells were continuously fed with 50 µL BE6.2 media plus 1% matrigel plus 3µM of IWR-1e in each well. On day 4 and -5, cells were fed with 100 µLs fresh BE6.2 media plus 1% matrigel plus 3µM of IWR-1e after removing 100µL of old media from each well. On day 6 IWR-1e and matrigel was no longer fed and placed in normoxia (5% $CO_2$, 21% $O_2$) incubator. Cells were then fed every other day with 100 µL BE6.2 media with 300 nM SAG until day 12 when cells were transferred to non-tissue culture polystyrene 10 cm dishes (aka bacterial grade plates) and kept feeding with 15ml BE6.2 media with 300nM SAG until day 14. Neural vesicles were excised on day 12. On day 14 cells were switched to 15ml LTR media consisted of 125 mL F12 (Gibco), 50 mL 100% FCS (Gibco), 10 mL B27 with Vitamin A (ThermoFischer), 5 mL Glutamax 100X (Gibco), 5 mL NEAA 100X (Gibco), 5 mL Sodium Pyruvate 100X (Gibco), 5mL Antibiotic-Antimyotic 100X (ThermoFischer) 500 µL 1M stock taurine (Sigma-Aldrich) in DMSO (Sigma-Aldrich) and brought to 500ml using DMEM high

glucose) with 300nM SAG. On day 18 cells were no longer treated with SAG. On day 20 cells were treated with 500nM ATRA (Sigma-Aldrich) until day 120.

**Cultivation of Müller cells from differentiated 3D organoids.** 2 organoids at age of d60-d90 were collected and washed with 5ml dPBS buffer (Thermo Fischer). 1mL of accumax (Gibco) were added to disassociate organoids. The organoids were incubated under 37°C for 20 minutes before washed with 5mL of dPBS and 1ml of Müller Cell Media consisted of 440mL DMEM high glucose media (Gibco), 50ml 100% FBS (Gibco), 5ml NEAA 100X (Gibco), and 5ml Sodium Pyruvate 100X (Gibco) twice. To further disassociate organoids, 1000μL wide orifice filter tips (VWR) were used to gently pipet up and down the cells before switched to regular P1000 tips and triturated again gently for 10-20 times. The disassociated cells were plated at approximately 1,000,000 cells/cm² on a matrigel-coated 24 well TC treated plate (USA Scientific).

**Fixing Cryoembedding and Cryosectioning of 3D organoids.** 1-5 organoids at age of d60-90 were collected and washed with 1ml dPBS buffer (Thermo Fischer) three times before incubation in cold fixation buffer (4% Paraformaldehyde (Thermo Fischer), 5% sucrose (Sigma-Aldrich) in 0.1M Sorrenson's Buffer (Electro Microscopy Science)) for 1 hour and 30 minutes at room temperature. The organoids were then rinsed at least 3 times with cool 5% sucrose in 0.1M phosphate buffer before incubated in 6.75% sucrose in 0.1M phosphate buffer at room temperature for 30 minutes. Then the organoids were incubated in 12.5% sucrose in 0.1M phosphate buffer for 30 minutes at room temperature. The organoids were incubated in 25% sucrose in 0.1M phosphate buffer at 4°C overnight. The next day, the organoids were transferred to OCT embedding media and sectioned to 10 microns under -20°C using a Leica cryostat.

**RNA extraction and Reverse-transcription into cDNA.** RNA was extracted from 2D dissociated *GLAST* H2B GFP organoid culture and 3D d90 *Brn3b* H2B tdTomato *GLAST* H2B GFP IMR90.4 derived retinal organoid following Zymo Quick-RNA extraction kit (Zymo). The extracted RNA was reverse-transcribed into cDNA using SuperScript IV (Thermo Fischer). Reverse Transcriptase. The cDNA was then PCR amplified using primers spanning the introns of *GLAST, GLUL, GFAP, hRPL30* and *Brn3b*, which are listed below (Table 1).

Table 1. Primers used in cDNA PCR amplification

| *hRPL30* | F: ACAGCATGCGGAAAATACTAC |
|---|---|
| | R: AAAGGAAAATTTTGCAGGTT |
| *Brn3b* | F: GCTCGGAGGCTATGCGGAGA |
| | R: TGGTGGTGGTGGCTCTTGCT |
| *SLC1A3* | F: CCTGTTTCGGAATGCTTTTG |
| | R: CCATCTTCCCTGATGCCTTA |
| *GLUL* | F: TTGGCATGGAGCAGGAGTAT |
| | R: TCTGCTCCCACACCACAGTA |
| *GFAP* | F: AAAGAGATCCGCACGCAGTA |
| | R: GTAGTCGTTGGCTTCGTGCT |

## Acknowledgements

47

Reference

Agathocleous, M., and Harris, W.A. (2009). From Progenitors to Differentiated Cells in the
Vertebrate Retina. Annual Review of Cell and Developmental Biology *25*, 45–69.

Bhatia, B., Singhal, S., Jayaram, H., Khaw, P.T., and Limb, G.A. (2010). Adult Retinal Stem
Cells Revisited. Open Ophthalmol J *4*, 30–38.

Campbell, L.J., Willoughby, J.J., and Jensen, A.M. (2012). Two Types of Tet-On Transgenic
Lines for Doxycycline-Inducible Gene Expression in Zebrafish Rod Photoreceptors
and a Gateway-Based Tet-On Toolkit. PLoS One *7*.

Castanheira, P., Torquetti, L., Nehemy, M.B., and Goes, A.M. (2008). Retinal incorporation and
differentiation of mesenchymal stem cells intravitreally injected in the injured retina of
rats. Arq Bras Oftalmol *71*, 644–650.

Cerbini, T., Funahashi, R., Luo, Y., Liu, C., Park, K., Rao, M., Malik, N., and Zou, J. (2015).
Transcription Activator-Like Effector Nuclease (TALEN)-Mediated CLYBL Targeting
Enables Enhanced Transgene Expression and One-Step Generation of Dual Reporter
Human Induced Pluripotent Stem Cell (iPSC) and Neural Stem Cell (NSC) Lines.
PLoS One *10*.

Chao, J.R., Lamba, D.A., Klesert, T.R., Torre, A.L., Hoshino, A., Taylor, R.J., Jayabalu, A.,
Engel, A.L., Khuu, T.H., Wang, R.K., Neitz, M., Neitz, J., Reh, T.A. (2017).
Transplantation of Human Embryonic Stem Cell-Derived Retinal Cells into the
Subretinal Space of a Non-Human Primate. Transl Vis Sci Technol *6*.

Fischer, A.J. (2011). Müller Glia, Vision-Guided Ocular Growth, Retinal Stem Cells, and a Little
Serendipity: The Cogan Lecture. Invest. Ophthalmol. Vis. Sci. *52*, 7705–7710.

Goldman, D. (2014). Müller glial cell reprogramming and retina regeneration. Nature Reviews
Neuroscience *15*, 431–442.

Hojo, M., Ohtsuka, T., Hashimoto, N., Gradwohl, G., Guillemot, F., and Kageyama, R. (2000).
Glial cell fate specification modulated by the bHLH gene Hes5 in mouse retina.
Development *127*, 2515–2522.

Kim, J.H., Lee, S.-R., Li, L.-H., Park, H.-J., Park, J.-H., Lee, K.Y., Kim, M.-K., Shin, B.A., and
Choi, S.-Y. (2011). High Cleavage Efficiency of a 2A Peptide Derived from Porcine
Teschovirus-1 in Human Cell Lines, Zebrafish and Mice. PLOS ONE *6*, e18556.

Llonch, S., Carido, M., and Ader, M. (2018). Organoid technology for retinal repair.
Developmental Biology 433, 132–143.

López-Colomé, A.M., López, E., Mendez-Flores, O.G., and Ortega, A. (2016). Glutamate
Receptor Stimulation Up-Regulates Glutamate Uptake in Human Müller Glia Cells.
Neurochem. Res. *41*, 1797–1805.

Marquardt, T., and Gruss, P. (2002). Generating neuronal diversity in the retina: one for nearly
all. Trends in Neurosciences *25*, 32–38.

Nichols, J. (2001). Introducing embryonic stem cells. Current Biology *11*, R503–R505.

Oberdoerffer, P., Otipoby, K.L., Maruyama, M., and Rajewsky, K. (2003). Unidirectional Cre-
mediated genetic inversion in mice using the mutant loxP pair lox66/lox71. Nucleic
Acids Res *31*, e140.

Ooto, S., Akagi, T., Kageyama, R., Akita, J., Mandai, M., Honda, Y., and Takahashi, M. (2004).
Potential for neural regeneration after neurotoxic injury in the adult mammalian retina.
Proc Natl Acad Sci U S A *101*, 13654–13659.

Pellissier, L.P., Hoek, R.M., Vos, R.M., Aartsen, W.M., Klimczak, R.R., Hoyng, S.A., Flannery, J.G., and Wijnholds, J. (2014). Specific tools for targeting and expression in Müller glial cells. Mol Ther Methods Clin Dev *1*, 14009.

Qiu, F., Jiang, H., and Xiang, M. (2008). A Comprehensive Negative Regulatory Program Controlled by Brn3b to Ensure Ganglion Cell Specification from Multipotential Retinal Precursors. J Neurosci *28*, 3392–3403.

Rico, E., Jeacock, L., Kovářová, J., and Horn, D. (2018). Inducible high-efficiency CRISPR-Cas9-targeted gene editing and precision base editing in African trypanosomes. Scientific Reports *8*, 7960.

Tak, Y.E., Kleinstiver, B.P., Nuñez, J.K., Hsu, J.Y., Horng, J.E., Gong, J., Weissman, J.S., and Joung, J.K. (2017). Inducible and multiplex gene regulation using CRISPR-Cpf1-based transcription factors. Nat. Methods *14*, 1163–1166.

Takahashi, K., and Yamanaka, S. (2006). Induction of Pluripotent Stem Cells from Mouse Embryonic and Adult Fibroblast Cultures by Defined Factors. Cell *126*, 663–676.

Vecino, E., Rodriguez, F.D., Ruzafa, N., Pereiro, X., and Sharma, S.C. (2016). Glia–neuron interactions in the mammalian retina. Progress in Retinal and Eye Research *51*, 1–40.

Wahlin, K.J., Maruotti, J.A., Sripathi, S.R., Ball, J., Angueyra, J.M., Kim, C., Grebe, R., Li, W., Jones, B.W., and Zack, D.J. (2017). Photoreceptor Outer Segment-like Structures in Long-Term 3D Retinas from Human Pluripotent Stem Cells. Scientific Reports *7*, 766.

Walcott, J.C., and Provis, J.M. (2003). Müller cells express the neuronal progenitor cell marker nestin in both differentiated and undifferentiated human foetal retina. Clinical & Experimental Ophthalmology *31*, 246–249.

Wan, J., Zheng, H., Chen, Z.-L., Xiao, H.-L., Shen, Z.-J., and Zhou, G.-M. (2008). Preferential regeneration of photoreceptor from Müller glia after retinal degeneration in adult rat. Vision Research *48*, 223–234.

Yao, K., Qiu, S., Wang, Y.V., Park, S.J.H., Mohns, E.J., Mehta, B., Liu, X., Chang, B., Zenisek, D., Crair, M.C., Demb, J.B., Chen, B. (2018). Restoration of vision after de novo genesis of rod photoreceptors in mammalian retinas. Nature *560*, 484.

Zhong, X., Gutierrez, C., Xue, T., Hampton, C., Vergara, M.N., Cao, L.-H., Peters, A., Park, T.S., Zambidis, E.T., Meyer, J.S., Gamm, D.M., Yau, K.W., Canto-Soler, M.V. (2014). Generation of three-dimensional retinal tissue with functional photoreceptors from human iPSCs. Nature Communications *5*, 4047.

Zhou, Y., and Danbolt, N.C. (2013). GABA and Glutamate Transporters in Brain. Front Endocrinol (Lausanne) *4*.

Zolessi, F.R., Poggi, L., Wilkinson, C.J., Chien, C.-B., and Harris, W.A. (2006). Polarization and orientation of retinal ganglion cells in vivo. Neural Develop *1*, 2.